Histol Histopathol (2012) 27: 1559-1577
DOI: 10.14670/HH-27.1559

http://www.hh.um.es

Histology and Histopathology
Cellular and Molecular Biology

Proposed mechanism in the change of cellular composition in the outer medullary collecting duct during potassium homeostasis

Eun-Young Park[1], Wan-Young Kim[1], Yu-Mi Kim[1], Jeong-Hwa Lee[2], Ki-Hwan Han[3], I. David Weiner[4] and Jin Kim[1]

[1]Department of Anatomy and Cell Death Disease Research Center, College of Medicine, The Catholic University of Korea, Seoul, Korea, [2]Department of Biochemistry, College of Medicine, The Catholic University of Korea, Seoul, Korea, [3]Department of Anatomy, Ewha Womans University, Seoul, Korea and [4]Division of Nephrology, Hypertension, and Transplantation, University of Florida, Gainesville, Florida, USA

Summary. Potassium depletion (K^+-D) induces hypertrophy and hyperplasia of collecting duct cells, and potassium repletion (K^+-R) induces regression of these changes. The purpose of this study was to examine the time courses of the changes in cellular composition, the origin of intercalated cells (ICs) and the mechanism responsible for these changes. SD rats received K^+-depleted diets for 1, 7, or 14 days. After K^+-D for 14 days some of the rats received normal diets for 1, 3, 5, or 7 days. In the inner stripe of the outer medulla, K^+-D increased significantly the number and proportion of H^+-ATPase-positive ICs, but decreased the proportion of H^+-ATPase-negative principal cells (PCs). However, proliferation was limited to H^+-ATPase-negative PCs. During K^+-R, the cellular composition was recovered to control level. Apoptosis increased during K^+-R and exclusively limited in H^+-ATPase-negative PCs. Double immunolabeling with antibodies to PC and IC markers identified both cells negative or positive for all markers during both K^+-D and K^+-R. Electron microscopic observation showed that ultrastructure of AE1-positive some cells were similar to AE1-negative some cells during K^+-R. LC3 protein expression increased significantly and autophagic vacuoles appeared particularly in PCs on days 14 of K^+-D and in ICs on days 3 of K^+-R. These results suggest that PCs and ICs may interconvert in response to changes in dietary K^+ availability and that autophagic pathways may be involved in the interconversion.

Offprint requests to: Jin Kim, M.D., Ph.D., Department of Anatomy and Cell Death Disease Research Center, College of Medicine, The Catholic University of Korea, Seoul, Korea, 505, Banpo-Dong, Seocho-Ku, Seoul 137-701, Korea. e-mail: jinkim@catholic.ac.kr

Key words: Interconversion, Intercalated cell, Principal cell, Potassium-homeostasis, Autophagy

Introduction

The renal collecting duct (CD) consists of principal cells (PCs) and intercalated cells (ICs), which differ in function and structure: ICs are involved in acid-base balance, whereas PCs are involved in hormonally regulated reabsorption of sodium and water. Both cell types, ICs and PCs, are involved in potassium homeostasis; PCs through their role in potassium secretion and ICs through their ability to facilitate potassium reabsorption (Muto, 2001; Giebisch et al., 2003).

Potassium depletion induces profound effects in the kidney, and these are most prominent in the CD, particularly in the inner stripe of the outer medulla (ISOM) (Ordonez et al., 1977; Toyoshima and Watanabe, 1988). There is induction of hypertrophy, both in total ISOM volume and in ICs and PCs (Elger et al., 1992). In addition, there is evidence of hyperplasia, with some studies indicating increased numbers of ISOM cells, and there is evidence in some, but not all studies, for differential effects of hypokalemia on the cellular composition of ICs and PCs. In particular, K^+-depletion (K^+-D) increases the number and proportion of ICs that exhibit tight apical H^+-ATPase staining in the CD (Bailey et al., 1998; Silver et al., 2000). During K^+-D, cell proliferation increases markedly in the cortex, outer medulla (OM), and inner medulla (IM) (Kimura et al., 2001). These changes disappear rapidly after K^+-repletion (K^+-R). Correction of the hypokalemia not

only results in normalization of the hypertrophy, it also results in a transient reactivation of apoptosis which quickly self-terminates (Kimura et al., 2001). Previous studies have reached varying conclusions with regards to changes in the proportion of ICs and PCs in the ISOM, with some finding an increase in the relative number of ICs (Oliver et al., 1957; Toback et al., 1976) and others finding no significant changes (Hansen et al., 1980; Stetson et al., 1980).

The purpose of the current study was to reexamine the effects of hypokalemia followed by its correction on the ICs and PCs in the ISOM. We first determined the effect of hypokalemia and its correction on the cellular composition of ICs and PCs in the ISOM. We then examined whether these changes were due to proliferation and/or apoptosis of ICs or PCs. Because we identified an increased number and proportion of ICs with hypokalemia, but evidence of proliferation only in PCs, and that correction of hypokalemia decreased the number and proportion of ICs, but induced apoptosis primarily in PCs, we determined whether there was evidence for either an 'intermediate cell', expressing phenotypic characteristics of both ICs (H^+-ATPase and anion exchanger 1, AE1 immunoreactivity) and PCs (aquaporin 2, AQP2 immunoreactivity), or for a 'null cell', which expresses neither ICs nor PCs markers. Finally, we examined whether programmed autophagy contributed to changes in cell-type distribution in the ISOM. In the present study, we show new morphological evidence that PCs and ICs may convert to each other during potassium homeostasis. Also, we demonstrate that autophagic pathways may be involved in the interconversion between PCs and ICs.

Materials and methods

Experimental animals

The animal protocols were approved by the Animal Care and Use committee of The Catholic University of Korea. Male Sprague Dawley (SD, ORIENT BIO Inc., Gyeonggi, Korea) rats weighing 180-200 g were used. The animals were housed in metabolic cages. Urine output and water intake were measured for 24 h before the rats were sacrificed. The tissue preservation method has been described previously (Kim et al., 2006; Lee et al., 2007).

Protocol

The rats were divided into three groups. The K^+-depletion (K^+-D) group were given a potassium free diet (K^+; 0 gm, Research Diets Inc., New Brunswick, NJ, USA) for 1, 7, or 14 days (groups K^+-D1-14; n=5 per subgroup). The K^+-repletion (K^+-R) groups were fed a potassium-free diet for the first 14 days, and then a normal diet (K^+; 25 gm, Research Diets Inc.) for 1, 3, 5, or 7 days thereafter (groups K^+-R1-7; n=5 per subgroup). The control group was fed a normal diet throughout the trail (n=21). An intraperitoneal injection of 50 mg/kg body weight BrdU (Roche Ltd, Basel, Switzerland) was administered four times at 8 h intervals over 24 h before the animals were sacrificed, and the kidneys were preserved 2 h after the last injection of

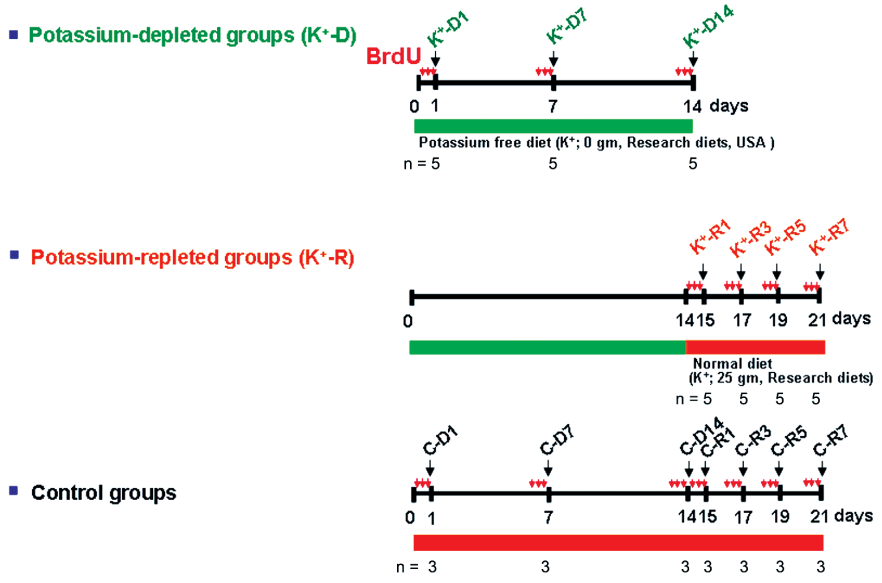

Fig. 1. Division into three groups for experimental protocol. ↓: Timing of sacrifice; n: number of rats in each subgroups, ↓↓↓: intraperitoneal injection of BrdU was administered four times at 8 h intervals during a total period of 24 h before the animals were sacrificed, and the kidneys were preserved 2 h after the last injection of BrdU.

BrdU (Fig. 1).

Antibodies

Aquaporin 2 (AQP2), a marker for PCs, was detected using a rabbit polyclonal antibody against AQP2 (Chemicon Inc., Temecula, CA), and goat polyclonal antibody against AQP2 (Abcam, Cambridge, UK). H^+-ATPase, a marker for ICs, was detected using a rabbit polyclonal antibody against human vacuolar-type H^+-ATPase B1 (V-ATPase B1; Santa Cruz Biotechnology, Santa Cruz, CA). The band-3-like Cl^-/HCO_3^- exchanger, a marker for ICs, was detected using a rabbit polyclonal antibody against rat AE1 (Alpha Diagnostic, San Antonio, TX). Cell proliferation was detected using a monoclonal antibody against BrdU (DakoCytomation, Glostrup, Denmark) and a polyclonal antibody against PCNA (Abcam, Cambridge, UK). Apoptosis was detected using an in situ TUNEL technique and a TdT-FragEL DNA fragmentation detection kit (Calbiochem Inc., Darmstadt, Germany). Autophagy was detected using a polyclonal antibody against LC3B (Sigma-Aldrich Inc., St. Louis, MO).

Light microscopic immunohistochemistry

Post-embedding method for single or double labeling

Single labeling. Wax-embedded 4 μm sections were incubated with AQP2 (1:2000) or H^+-ATPase (1:200) overnight at 4°C. The sections were then incubated for 2 h with an Envision kit (Dako), and labeling was visualized with 3,3'-diaminobenzidine (DAB, Sigma-Aldrich Inc.).

Double labeling. Wax-embedded 4 μm sections were processed for double immunolabeling with BrdU and H^+-ATPase or TUNEL and H^+-ATPase. To detect cell proliferation sections were incubated with BrdU (1:100) and labeling was visualized using DAB. The sections were then treated with methanolic H_2O_2 for 30 min to remove any peroxidase remaining from the first staining. The sections were incubated with the second primary antibody against H^+-ATPase (1:100) to detect ICs, and labeling was visualized with Vector SG (Vector Laboratories, Burlingame, CA), which produces a gray-blue color. To detect apoptosis, sections were analyzed using an in situ TUNEL technique and a TdT-FragEL DNA fragmentation detection kit.

Pre-embedding method for single labeling or double labeling

Fifty-micron vibratome sections were processed for immunohistochemistry using indirect pre-embedding immunoperoxidase methods and antibodies against AQP2 (1:2000) and AE1 (1:200) as previously described (Kim et al., 1994, 1999, 2002). Flat-embedded 50 μm vibratome sections prepared for single immunolabeling against AQP2 or AE1 were processed for double immunolabeling (H^+-ATPase and AE1, AQP2 and H^+-ATPase, or AQP2 and PCNA) using an indirect post-embedding immunoperoxidase method as reported previously (Song et al., 2007).

Confocal Microscopic Immunofluorescence

The procedure was the same as that used in the pre-embedding method before treatment with primary antibodies. For double immunofluorescence, goat anti-AQP2 antibody (1:500) was mixed with rabbit anti-H^+-ATPase antibody (1:200). Labeling was visualized using Alexa 488-conjugated donkey anti-rabbit antibody (1:300, Molecular Probes, Eugene, OR) and Cy3-conjugated donkey anti-goat antibody (1:500, Jackson ImmunoResearch Laboratories West Grove, PA). Tissues were mounted in Vectashield mounting media (Vector Laboratories). Images were acquired using a Zeiss LSM 510 confocal microscope (Carl Zeiss) and LSM 510 version 2.02 software.

Electron microscopic immunohistochemistry

Fifty-micron vibratome sections were prepared with an antibody against AE1 (1:200) for electron microscopic immunohistochemistry using indirect pre-embedding immunoperoxidase methods as reported (Kim et al., 2008).

Immunoblotting

Kidney tissues were dissected into their OM and IM constituents and homogenized in a glass tissue grinder in ice-cold isolation buffer (10 mM triethanolamine, 250 mM sucrose, 1 μg/ml leupeptin, and 2 mg/ml PMSF), after which SDS was added to a final concentration of 1% for western blot analysis of the total cell lysate. The protein concentration was determined using a modified Lowry method (Bio-Rad DC protein assay reagent, Bio-Rad, Richmond, CA). Proteins were separated using SDS-PAGE and 10% polyacrylamide gels and electrotransferred to polyvinylidene difluoride membranes (Bio-Rad) at 100 mV for 1 h. The membranes were incubated with primary antibodies diluted in 5% nonfat powdered milk in Tris-buffered saline containing Tween 20 (TBST; 0.2 M Tris, 1.37 M NaCl, 0.5% Tween 20, pH 7.6) at 4°C overnight. The membranes were treated for 2 h at room temperature with horseradish peroxidase-coupled goat anti-rabbit IgG (Bio-Rad), which was diluted in 5% nonfat powdered milk in TBST to a final dilution of 1:3000. The blots were detected using a western blotting luminol reagent kit (Santa Cruz Biotechnology).

Cell counting

Cell counting of the ISOM and IMi samples was

performed during protocol. The numbers of positive (labeled) and negative (unlabeled) cells with a distinct nucleus were counted. The numbers and densities of cells were divided by the length of the tubules for which counting was performed and are expressed per millimeter.

Statistics

Values are presented as mean ± SD. Data were compared between groups using an unpaired t test and Microsoft Excel 2003. P values less than 0.05 were considered significant.

Results

Functional studies

Dietary K^+-D and K^+-R caused substantial functional changes. Kidney weight, measured in the left kidney and expressed relative to total weight, increased significantly with K^+-D, with significant changes observed even on the first day of K^+-D, and these changes rapidly reversed with K^+-R. Similarly, K^+-D and K^+-R induced reversible polyuria and hypokalemia, but did not significantly alter urinary sodium excretion and serum sodium concentration. Metabolic alkalosis developed during K^+-D, as was evidenced by a higher plasma pH than the controls, and gradually recovered during K^+-R. All of these findings are consistent with expected changes in response K^+-D and K^+-R (Table 1).

Changes in cellular composition during K^+-D and K^+-R

Because ICs and PCs are believed to mediate different roles in potassium homeostasis, potassium secretion by PCs and potassium reabsorption by ICs, we examined whether K^+-D and K^+-R would alter either the number or proportion of these two different CD cell types in the ISOM and initial part of inner medulla (IMi). We used immunohistochemistry and identified ICs as H^+-ATPase-positive cells and PCs as AQP2-positive cells. AQP2-positive PCs and H^+-ATPase-positive ICs were hypertrophic during K^+-D but recovered during K^+-R (Fig. 2). The total cell number in tissue sections arising from cell hypertrophy decreased slightly during K^+-D, but the difference was not significant (975.60±90.70 vs. 1019.67±114.55; K^+-D14 vs. Control, not shown). However, the relative cell number per unit length increased significantly during K^+-D (Fig. 3B). The relative number of H^+-ATPase-positive ICs increased significantly on days 7 and 14 of K^+-D and decreased to control levels during K^+-R (Fig. 3A,B). The relative number of H^+-ATPase-negative PCs did not change significantly either during K^+-D or K^+-R (Fig. 3B). During K^+-D, the proportion of H^+-ATPase-positive ICs markedly increased, and the proportion of H^+-ATPase-negative PCs decreased significantly compared with control group (Fig. 3C). During K^+-R, the proportion of H^+-ATPase-positive ICs was significantly lower, and the proportion of H^+-ATPase-negative PCs was higher than K^+-D (Fig. 3C). Similar results were observed for the IMi (not shown).

Detection of cell proliferation

To investigate the role of cell proliferation in the increase in the number and proportion of ICs during K^+-D, we performed double immunolabeling with antibodies against BrdU and H^+-ATPase, or PCNA and AE1. In the ISOM, BrdU-positive cells peaked on day 7 of K^+-D and remained above control levels on day 14 of K^+-D. During K^+-R, there was a rapid decrease in BrdU-positive cells (Fig. 4I). Although the proportion of H^+-ATPase-positive ICs in the ISOM increased during K^+-D, the increase of proliferating cells, identified as BrdU-positivity, was limited to H^+-ATPase-negative PCs (Fig. 4C,D, arrows). Only rare BrdU-positive cells exhibited apical H^+-ATPase labeling (Fig. 4B,C, arrowheads), and BrdU-positive/H^+-ATPase-positive ICs did not change significantly as a result of either K^+-D or K^+-R (Fig. 4I).

PCNA expression was detected mainly in AQP2-positive/AE1-negative PCs (Fig. 5C-F, arrows), but was observed in some AQP2-negative/AE1-positive ICs during K^+-D (Fig. 5E,F, arrowheads). The number of PCNA-positive/AQP2-positive PCs increased

Table 1. Functional data for rats treated with potassium depletion (K^+-D) and repletion (K^+-R).

		K^+-D			K^+-R			
	Control (21)	1 (5)	7 (5)	14 (5)	1 (5)	3 (5)	5 m(5)	7 (5)
Left KW (g)/BW (g), x 10^{-3}	4.20±0.3	5.06±0.3*	5.60±0.2*	6.95±0.1*	5.56±05*	4.82±0.1*	4.39±0.4	4.29±0.4
Urine output, ml	6.17±2.02	17.00±2.65*	29.33±12.70*	27.33±5.05*	13.00±1.00*	8.33±0.58	7.00±1.73	7.33±1.15
Urine osmolality, mOsm/kgH_20	1389.67±28.54	889.67±110.50*	435.33±189.00*	616.67±73.82*	874.67±4.92*	1421.67±231.22	1442.00±338.39	1342.67±213.13
Urine K x Urine output, mmol	0.79±0.21	0.54±012	0.20±0.04*	0.19±0.09*	0.31±0.01*	0.40±0.08*	0.77±045	0.89±0.50
Urine Na x Urine output, mmol	0.57±0.14	0.57±0.08	0.38±0.07	0.42±0.06	0.37±0.06	0.51±0.18	0.54±0.29	0.46±0.10
Plasma K levels, mmol/l	4.57±0.55	4.23±0.35	3.07±0.40*	2.80±0.17*	3.90±0.10	5.37±0.12	5.35±0.35	5.03±0.38
Plasma Na levels, mmol/l	138.00±1.73	139.67±0.58	136.33±3.21	141.33±3.79	142.33±5.03	140.33±2.52	145.67±7.37	141.67±3.21
Blood pH	7.34±0.01	7.36±0.01	7.49±0.02*	7.51±0.02*	7.44±0.06	7.39±0.01	7.34±0.04	7.32±0.03

Values are expressed as the mean ± SE; n is indicated in parentheses. KW/BW, kidney weight per body weight. *: P<0.05

significantly between days 7 and 14 of K^+-D, but decreased gradually during K^+-R (Fig. 5I). However, numbers of PCNA-positive/AE1-positive ICs did not change significantly compared with the control group during K^+-D or K^+-R (Fig. 5I). Similar results were observed for the IMi (not shown). Thus, although K^+-D increased the total number and proportion of H^+-ATPase-/AE1-positive ICs, K^+-D increased cell proliferation mainly in AQP2-positive PCs.

Detection of cell removal

The lack of change in the proportion of PCs during K^+-D despite increased cell proliferation in PCs suggests either loss of PCs through cell removal or conversion of PCs to ICs. To begin examining these possibilities we next determined the role of apoptosis during K^+-D and K^+-R. During K^+-D, apoptotic, TUNEL-positive cells were only rarely identified, and quantification showed no significant change in either ICs, identified as H^+-ATPase-positive, TUNEL-positive cells, or in PCs, identified as H^+-ATPase-negative, TUNEL-positive cells. Thus, the decreased proportion of PCs during K^+-D despite evidence of PC proliferation is not due to parallel increases in PC apoptosis.

The decrease in the number and proportion of ICs during K^+-R suggests either loss of ICs through either apoptosis or cellular extrusion, or by conversion to PCs. To investigate the role of apoptosis in the change in ISOM cell populations during K^+-R we performed double labeling, using the TUNEL technique to identify cells actively undergoing apoptosis, and antibodies against H^+-ATPase to identify ICs. Many TUNEL-positive cells were observed on days 1, 3, and 5 of K^+-R, and double-immunolabel with antibodies to H^+-ATPase showed that the TUNEL-positive cells were PCs (Fig. 6C,D,F, arrows). Quantification showed that TUNEL-positive/H^+-ATPase-negative PCs were elevated significantly, and peaked on day 1 of K^+-R, remained elevated on day 3 and returned to baseline by day 5 of K^+-R (Fig. 6H). By day 7 of K^+-R, TUNEL-positive cells were not observed (Fig. 6G). Only rarely was TUNEL staining observed in H^+-ATPase-positive ICs during K^+-R, and quantification showed that TUNEL-positive/H^+-ATPase-positive ICs did not change significantly during K^+-R. Thus, the decrease in the number and proportion of ICs during K^+-R does not involve IC apoptosis.

A second mechanism used in the CD remodeling, at least during renal development, is extrusion of cells into the tubule lumen (Kim et al., 2000; Han et al., 2010). During K^+-R, we were able to identify removal of H^+-ATPase-negative PCs through 'extrusion' into the luminal space (Fig. 6D, arrowhead). Extruding H^+-ATPase-positive ICs was not observed, either during K^+-D or K^+-R.

Identification of 'Intermediate' and 'Null' CD cells during K^+-D and K^+-R

Changes in the number and proportion of ICs during K^+-D and K^+-R, but evidence of cellular proliferation

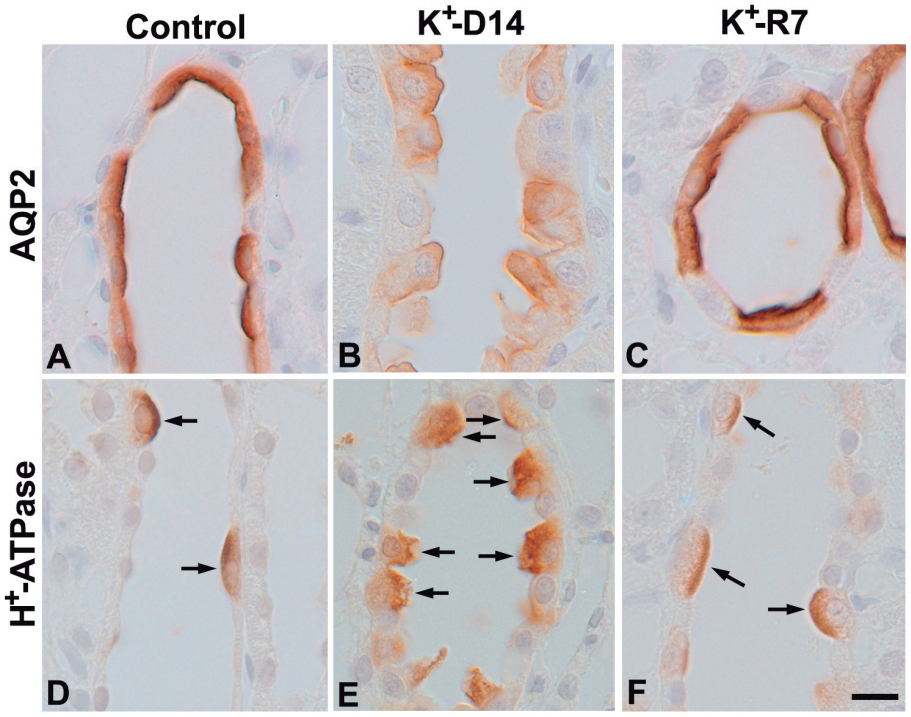

Fig. 2. Light micrographs of 4 μm wax sections of the inner stripe of the outer medulla (ISOM) of control **(A, D)**, K^+-D14 **(B, E)**, and K^+-R7 **(C, F)** rat kidneys illustrating single immunolabeling for AQP2 **(A-C)** and H^+-ATPase **(D-F)**. **B and E**. The collecting duct cells, AQP2-positive PCs and H^+-ATPase-positive ICs were hypertrophic, and the number of H^+-ATPase-positive ICs (arrows in **E**) increased markedly during K^+-D. During K^+-R the cells gradually recovered. Bar: 10 μm.

and apoptosis only in PCs, suggests the possibility of interconversion between ICs and PCs during K^+-D and K^+-R. To examine this possibility we examined whether 'intermediate' cells expressing phenotypic characteristics of both ICs and PCs, or 'null' cells, which do not express phenotypic characteristics of either ICs or PCs, were present. We used serial sections double-immunolabeled for either AQP2 and H^+-ATPase or AQP2 and AE1. Under control conditions, all ISOM cells exhibited either apical H^+-ATPase with basolateral AE1 (Fig. 7A,B, arrows) or apical AQP2 (Fig. 7A,B). However, during K^+-D, both 'null cells', negative for AQP2, H^+-ATPase, and AE1 (Fig. 7C,D, double arrows) and 'intermediate cells', positive for AQP2, H^+-ATPase, and AE1 (Fig. 7E,F, arrowheads) were present.

To confirm these findings further, we also repeated double immunolabeling in serial sections with antibodies to AE1 and AQP2, and to AE1 and H^+-ATPase. Similar changes were observed during K^+-R, both 'null cells', negative for AQP2, H^+-ATPase, and AE1 (Fig. 8D-F, double arrows) and 'intermediate cells', positive for AQP2, H^+-ATPase, and AE1 (Fig. 8G-I, arrowheads) were present.

In addition, we confirmed the existence of 'intermediate cells' and 'null cells' using double-immunofluorescence. Normally, AQP2 is expressed only in the apical portion of PCs (Fig. 9A-I, open arrowheads) and H^+-ATPase is expressed only in the apical portion of ICs (Fig. 9A-I, arrows). Some cells coexpressed AQP2, a marker for PCs, and H^+-ATPase, a marker for ICs, in the apical region on day 14 of K^+-D (Fig. 9D-F, arrowheads), whereas cells in control rats did not. Furthermore, a few 'null cells', negative for AQP2 and H^+-ATPase were evident on day 14 of K^+-D (Fig. 9, G-I, double arrows).

The results of cell counting are shown in detail in Table 2. The proportions of 'null cells' , negative for AQP2, H^+-ATPase, and AE1 and 'intermediate cells', positive for AQP2, H^+-ATPase, and AE1 on day 14 of K^+-D and day 3 of K^+-R accounted for 0.96% and 1.12% of the total cell proportion, respectively. However, these cells were not observed in the control

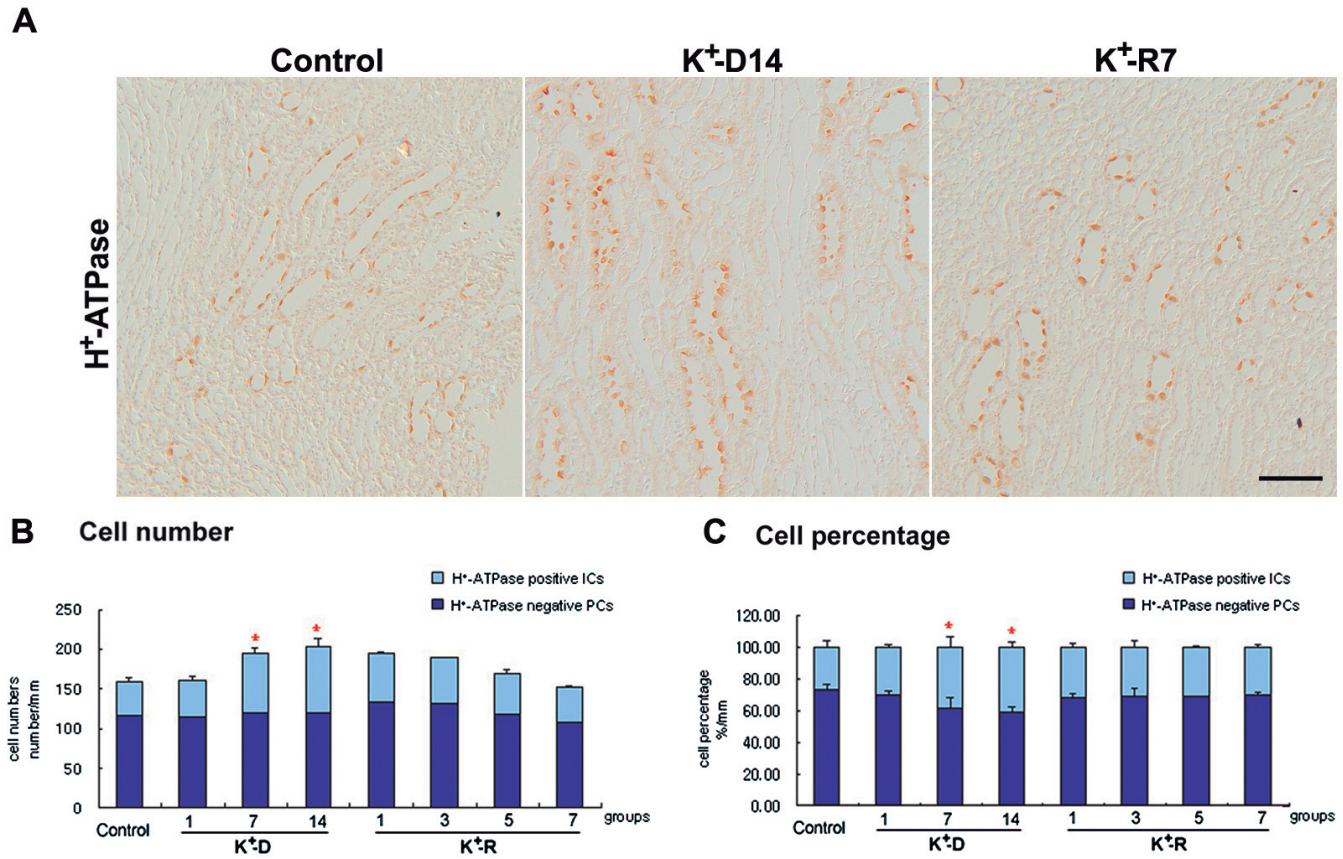

Fig. 3. Light micrographs of 4 μm wax sections in the inner stripe of outer medulla (ISOM) of control, K^+-D14, and K^+-R7 rat kidneys illustrating single immunolabeling for H^+-ATPase **(A)**. Quantification of the cell number **(B)** and proportion **(C)** in the ISOM of control, K^+-D, and K^+-R. A-C. During K^+-D the number and proportion of H^+-ATPase-positive ICs increased significantly. During K^+-R these changes rapidly decreased to those of the controls. *$P<0.05$ vs. control (B-C). Bar: 100 μm.

group.

Collecting duct ultrastructure during K^+-D and K^+-R

On day 14 of K^+-D, AE1-positive ICs were hypertrophied and exhibited well developed basolateral membrane compared with the control group (Fig. 10A,B), and AE1-negative PCs contained many intercellular vesicles (Fig. 10B, double arrows). In contrast, on day 3 of K^+-R, AE1 immunolabeling was very weak (Fig. 10C, arrows) and was present in the intracellular structures of some cells (Fig. 10D, arrowhead).

Ultrastructural examination with simultaneous AE1 immunolabel showed that on control diet AE1-positive ICs had prominent apical microplicae and numerous mitochondria in the cytoplasm and high levels of basolateral AE1 immunolabeling (Fig. 11A). Interestingly, on day 3 of K^+-R, the ultrastructure of a subpopulation of AE1-positive ICs exhibited weak basolateral AE1 immunolabeling and a cellular ultrastructure nearly identical to that of PCs (Fig. 11B). Thus, these cells had phenotypic characteristics of both ICs (AE1 immunolabel) and PCs (cellular

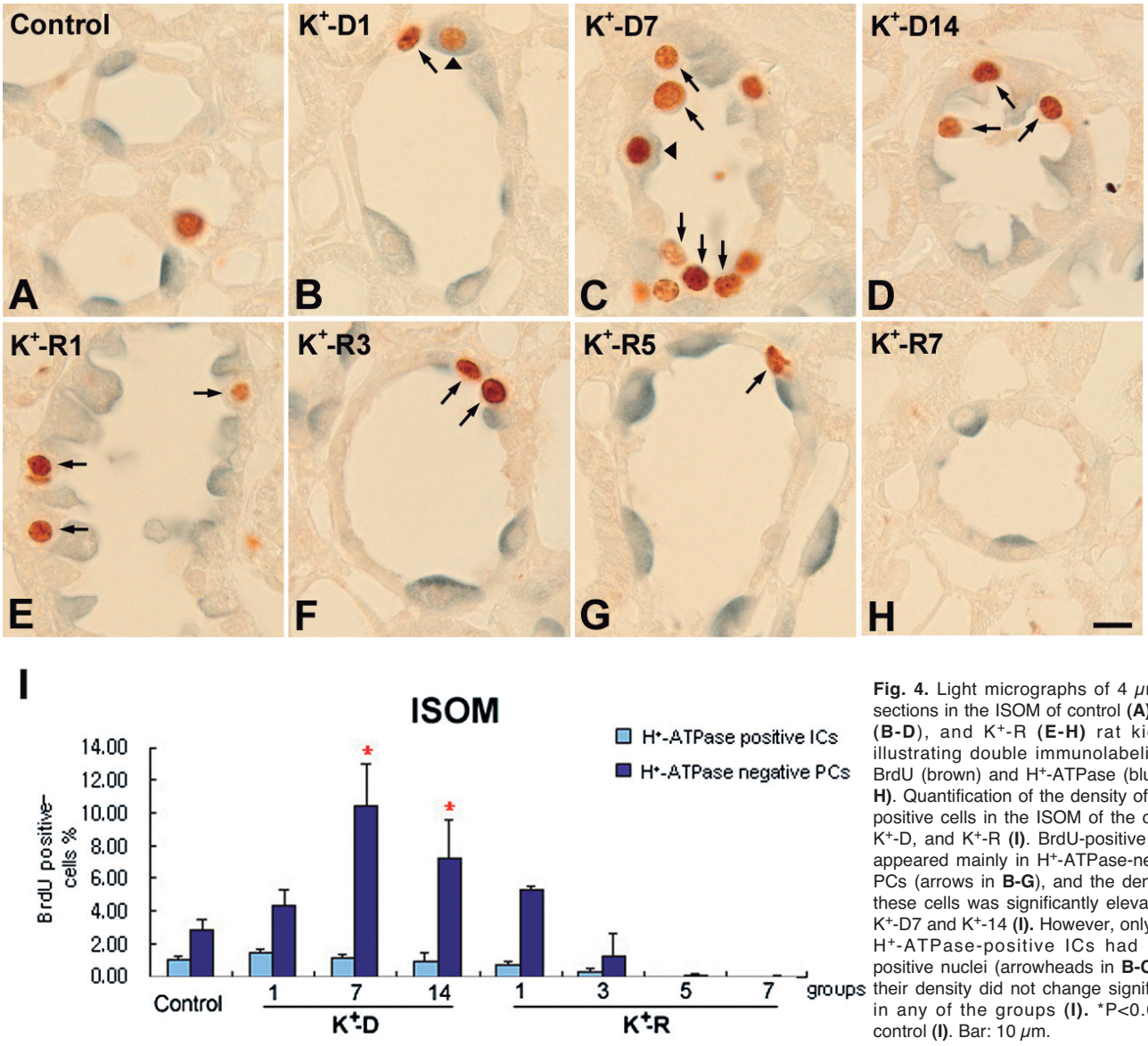

Fig. 4. Light micrographs of 4 μm wax sections in the ISOM of control **(A)**, K^+-D **(B-D)**, and K^+-R **(E-H)** rat kidneys illustrating double immunolabeling for BrdU (brown) and H^+-ATPase (blue) **(A-H)**. Quantification of the density of BrdU-positive cells in the ISOM of the control, K^+-D, and K^+-R **(I)**. BrdU-positive nuclei appeared mainly in H^+-ATPase-negative PCs (arrows in **B-G**), and the density of these cells was significantly elevated on K^+-D7 and K^+-14 **(I)**. However, only a few H^+-ATPase-positive ICs had BrdU-positive nuclei (arrowheads in **B-C**), and their density did not change significantly in any of the groups **(I)**. *$P<0.05$ vs. control **(I)**. Bar: 10 μm.

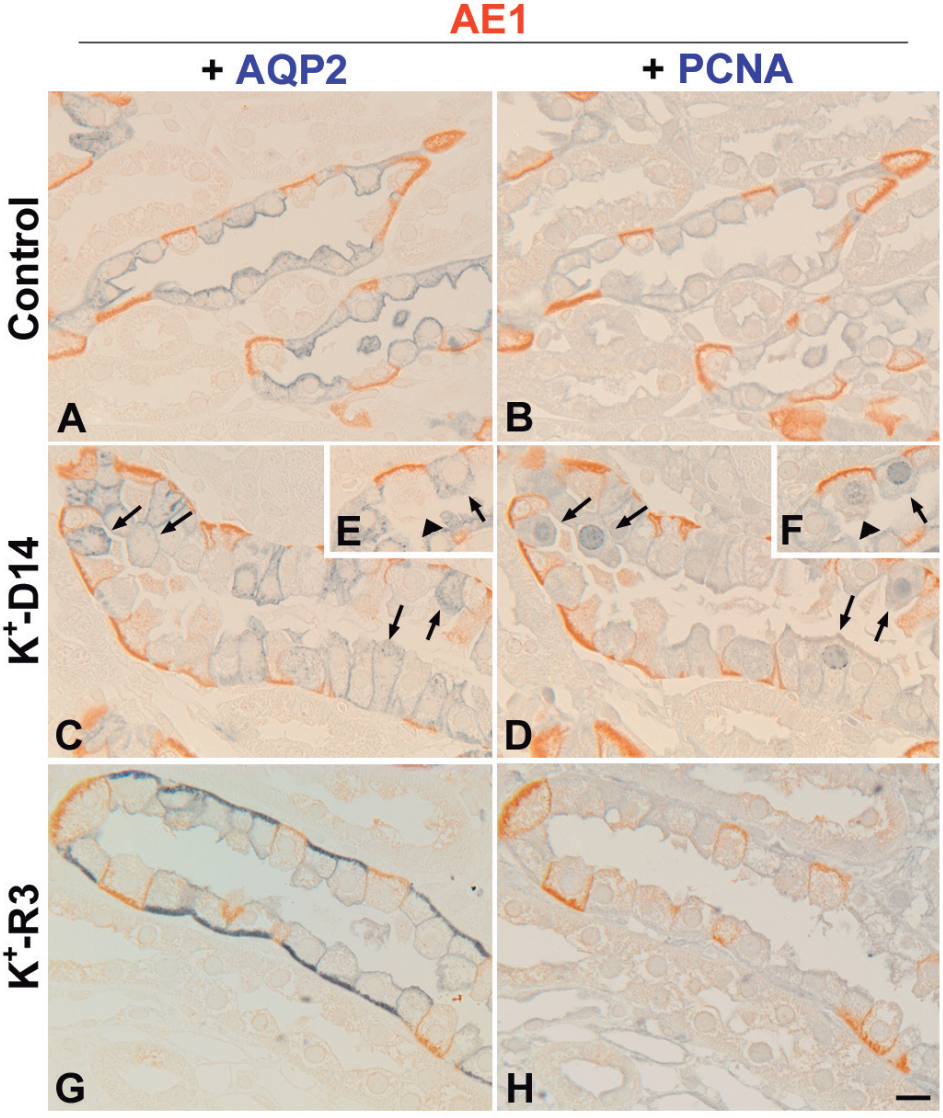

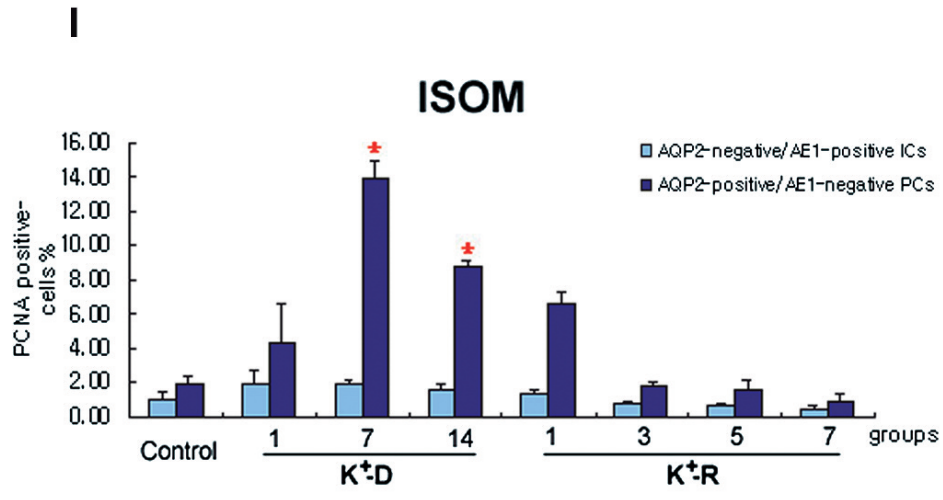

Fig. 5. Light micrographs of 1.5 μm semithin serial sections in the ISOM of control **(A-B)**, K^+-D14 **(C-F)**, and K^+-R3 **(G-H)** rat kidneys illustrating double immunolabeling for AE1 (brown) and AQP2 (blue in **A, C, E, G**), AE1 (brown) and PCNA (blue in **B, D, F, H**). Quantification of the density of PCNA-positive cells in the ISOM of the control, K^+-D, and K^+-R **(I).** Nuclear PCNA was mainly expressed in AQP2-positive/AE1-negative PCs (arrows in **C-F**), and the density of these cells was significantly elevated on K^+-D7 and K^+-D14. Although a few AQP2-negative/AE1-positive ICs with PCNA labeling were observed (arrowheads in **E-F**), their density did not change significantly during K^+-D or K^+-R **(I)**. *$P < 0.05$ vs. control **(I)**. Bar: 10 μm.

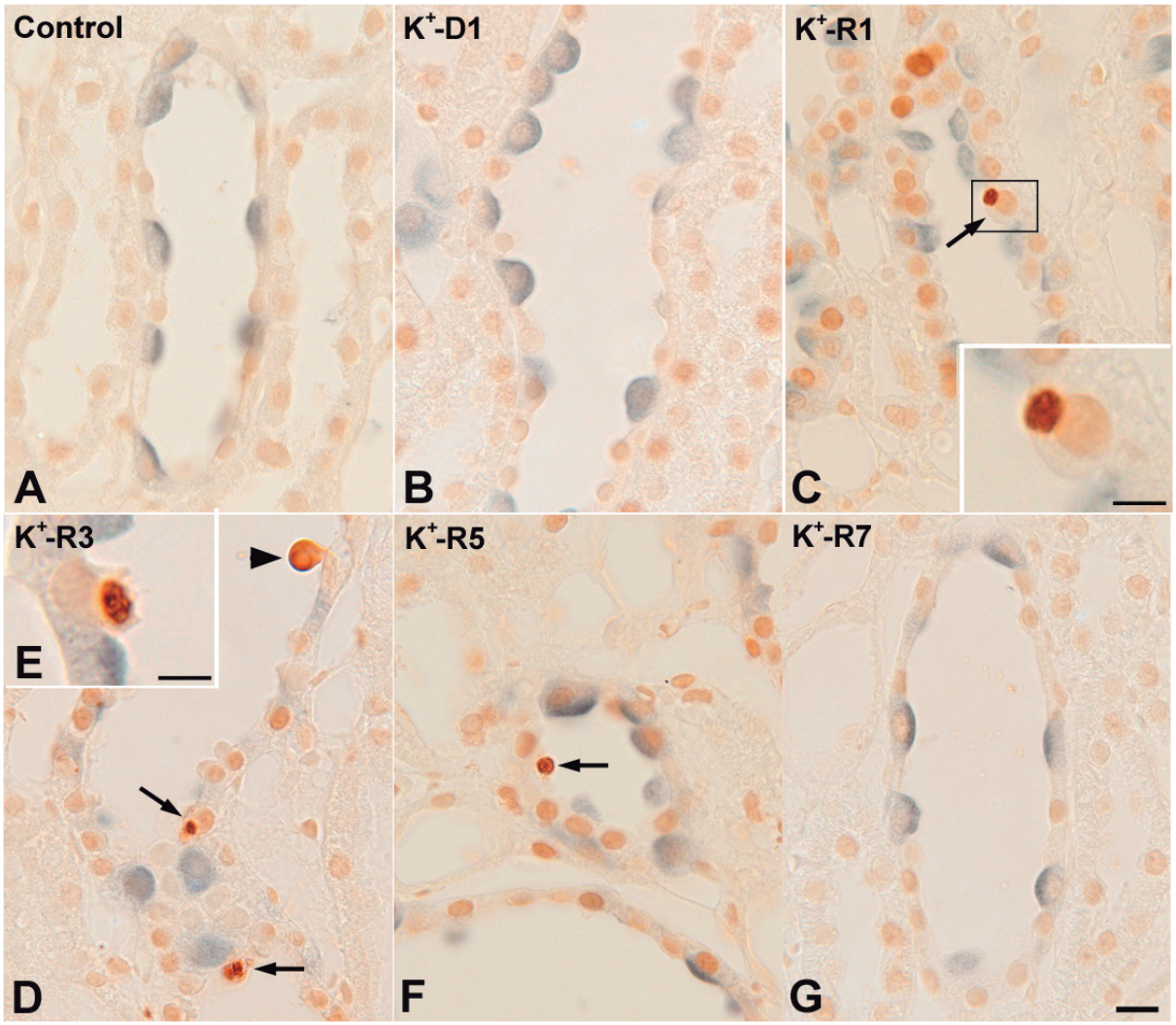

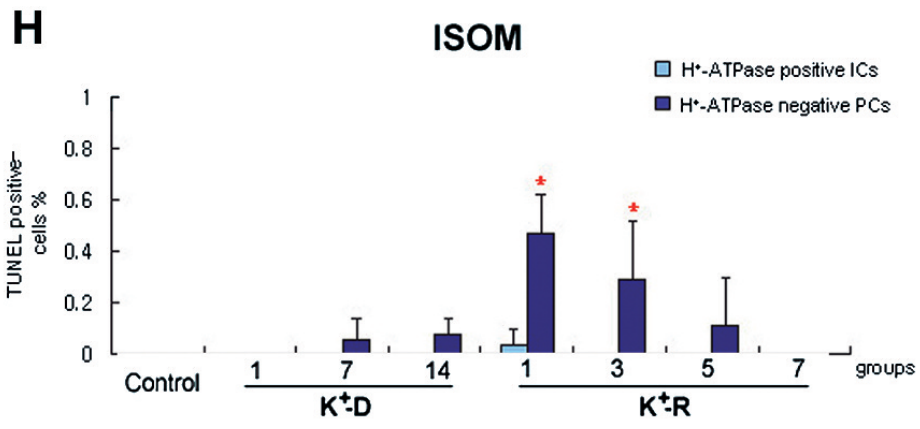

Fig. 6. Light micrographs of 4 μm wax sections in the ISOM of control **(A)**, K^+-D **(B)**, and K^+-R **(C-G)** rat kidneys illustrating double immunolabeling for TUNEL (brown) and H^+-ATPase (blue) **(A-G)**. Quantification of the density of TUNEL-positive cells in the ISOM of control, K^+-D, and K^+-R **(H)**. TUNEL-positive cells were not observed in the control **(A)**, K^+-D **(B)**, and K^+-R7 **(G)**. In contrast, a few TUNEL-positive nuclei appeared on K^+-R1 **(C)**, K^+-R3 **(D, E)**, and K^+-R5 **(F)**, mainly in H^+-ATPase-negative PCs (arrows in **C, D, F**), and the density of these cells was significantly elevated **(H)**. Note, cell death of H^+-ATPase-negative PCs occurred via removal, as well as via apoptosis (arrowhead in **D**). The inset panel is high-magnification of the marked areas in **C** (bar 5 μm). Phagocytosis of apoptotic cells was observed in H^+-ATPase-negative PCs **(E)**. Few TUNEL-positive cells consisted of H^+-ATPase positive IC and the density of these cells did not change significantly in any of the groups **(H)**. *$P<0.05$ **(H)**. Bars: A-D, F, G, 10 μm; E, 8 μm.

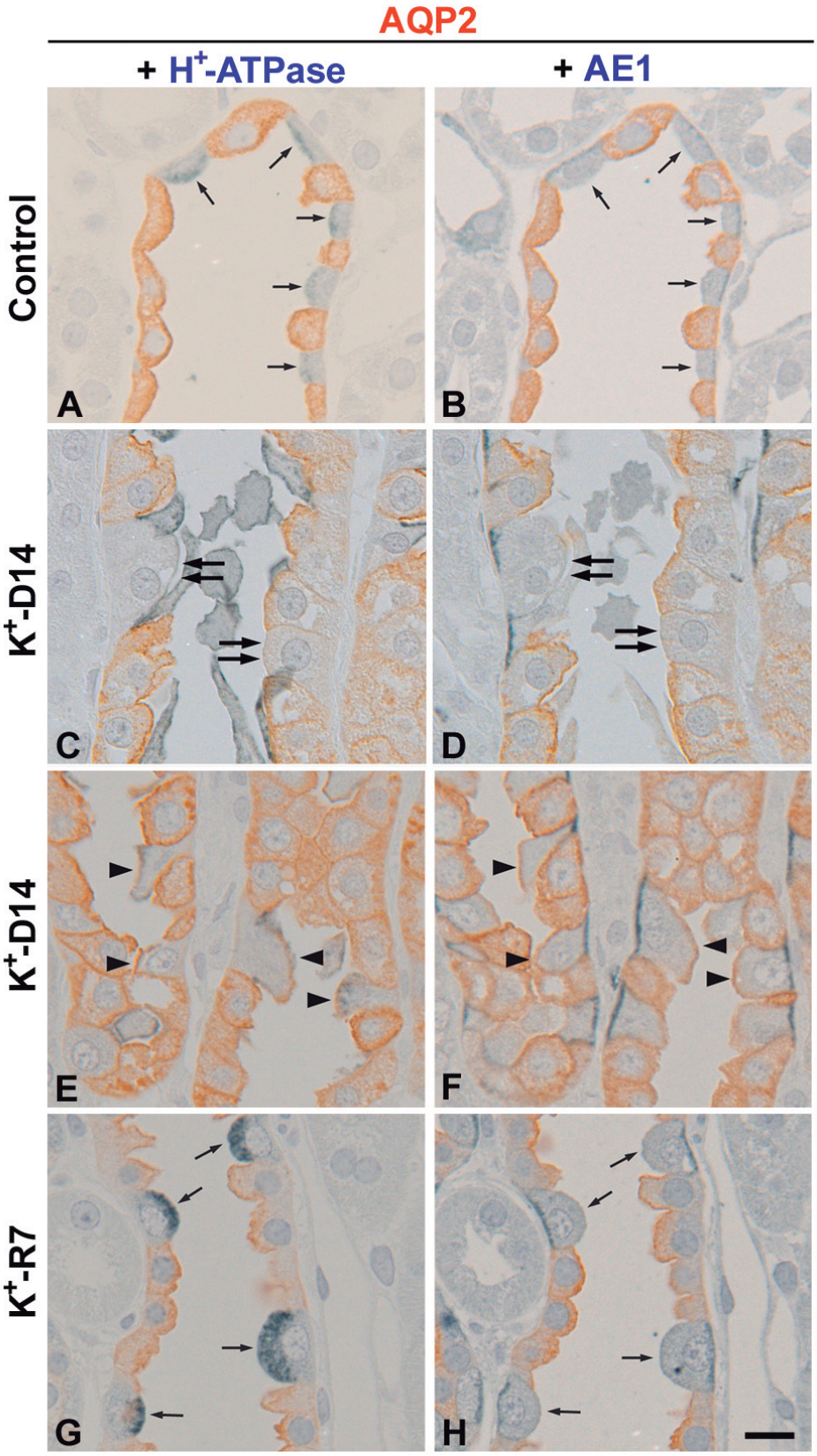

Fig. 7. Light micrographs of 1.5 μm semithin sections in the ISOM of control **(A-B)**, K^+-D14 **(C-F)**, and K^+-R7 **(G-H)** rat kidneys illustrating double immunolabeling for AQP2 (brown) and H^+-ATPase (blue in **A, C, E, G**), AQP2 (brown) and AE1 (blue in **B, D, F, H**). Type A ICs (arrows in **A, B, G, H**) exhibit apical H^+-ATPase immunolabeling and basolateral AE1 immunolabeling. However, some cells on K^+-D14 were all negative for AQP2, H^+-ATPase and AE1 (double arrows in **C-D**). Moreover, some cells exhibiting apical AQP2 and H^+-ATPase labeling on K^+-D14 exhibited AE1 immunolabeling of the basolateral plasma membrane (arrowheads in **E-F**). Bar: 10 μm.

ultrastructure).

Detection of autophagy during K⁺-D and K⁺-R

Autophagy is a conserved catabolic pathway that enables recycling of proteins through the lysosomal pathway. To investigate whether interconversion between ICs and PCs might involve autophagy, we examined expression of LC3 II, one of the key proteins involved in the initial development of autophagosomes

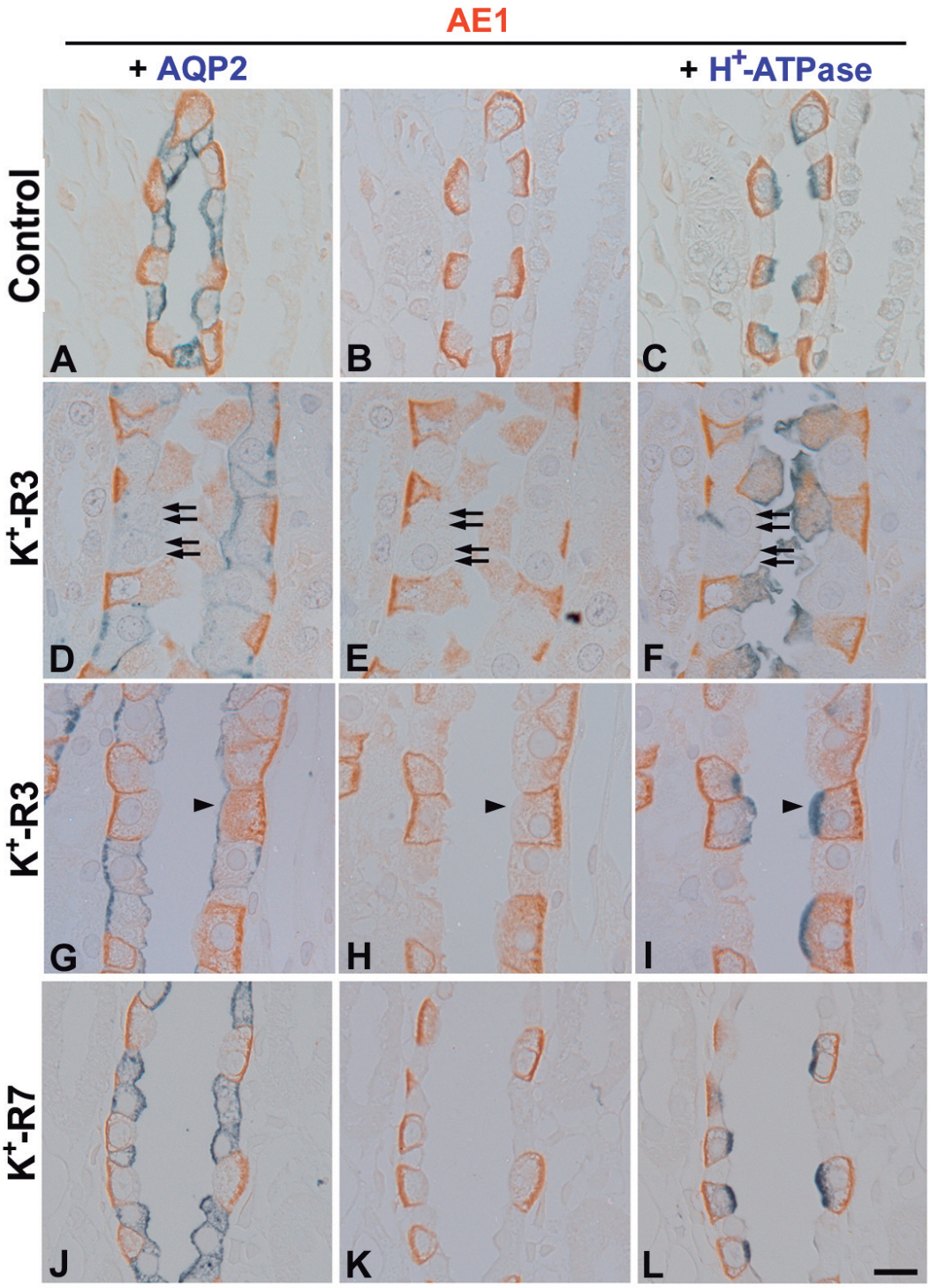

Fig. 8. Light micrographs of 1.5 μm semithin sections in the ISOM of control **(A-C)**, K⁺-R3 **(D-I)**, and K⁺-R7 **(J-L)** rat kidneys illustrating double immunolabeling for AE1 (brown) and AQP2 (blue in **A, D, G, J**) or H⁺-ATPase (blue in **C, F, I, L**). On K⁺-R3, some cells were negative for AQP2, H⁺-ATPase, and AE1 (double arrows in **D-F**). Interestingly, some cells on K⁺-R3 were positive for AQP2, H⁺-ATPase, and AE1 (arrowheads in **G-I**). Bar: 10 μm.

(Periyasamy-Thandavan et al., 2009). LC3 II expression was markedly increased in the OM and IM on day 7 of K^+-D and on day 3 of K^+-R (Fig. 12), suggesting induction of autophagy during both the response to K^+-D and K^+-R.

To confirm further the induction of autophagy in the ISOM, we used ultrastructural analysis to identify the presence and number of autophagic vacuoles (AVs). Immunoelectron microscopy showed that AE1-negative PCs contained many AVs on day 14 of K^+-D (Fig. 13A, B). On day 3 of K^+-R, AE1-positive ICs contained AVs (Fig. 13C, D, arrows) and multivesicular bodies (Fig. 13C, D, double arrows) in the cytoplasm. We identified that AVs in the ISOM were increased significantly in both number and volume on day 14 of K^+-D and on day 3 of K^+-R when compared with the control group. Interestingly, the number and volume of AVs were particularly pronounced in PCs on day 14 of K^+-D and

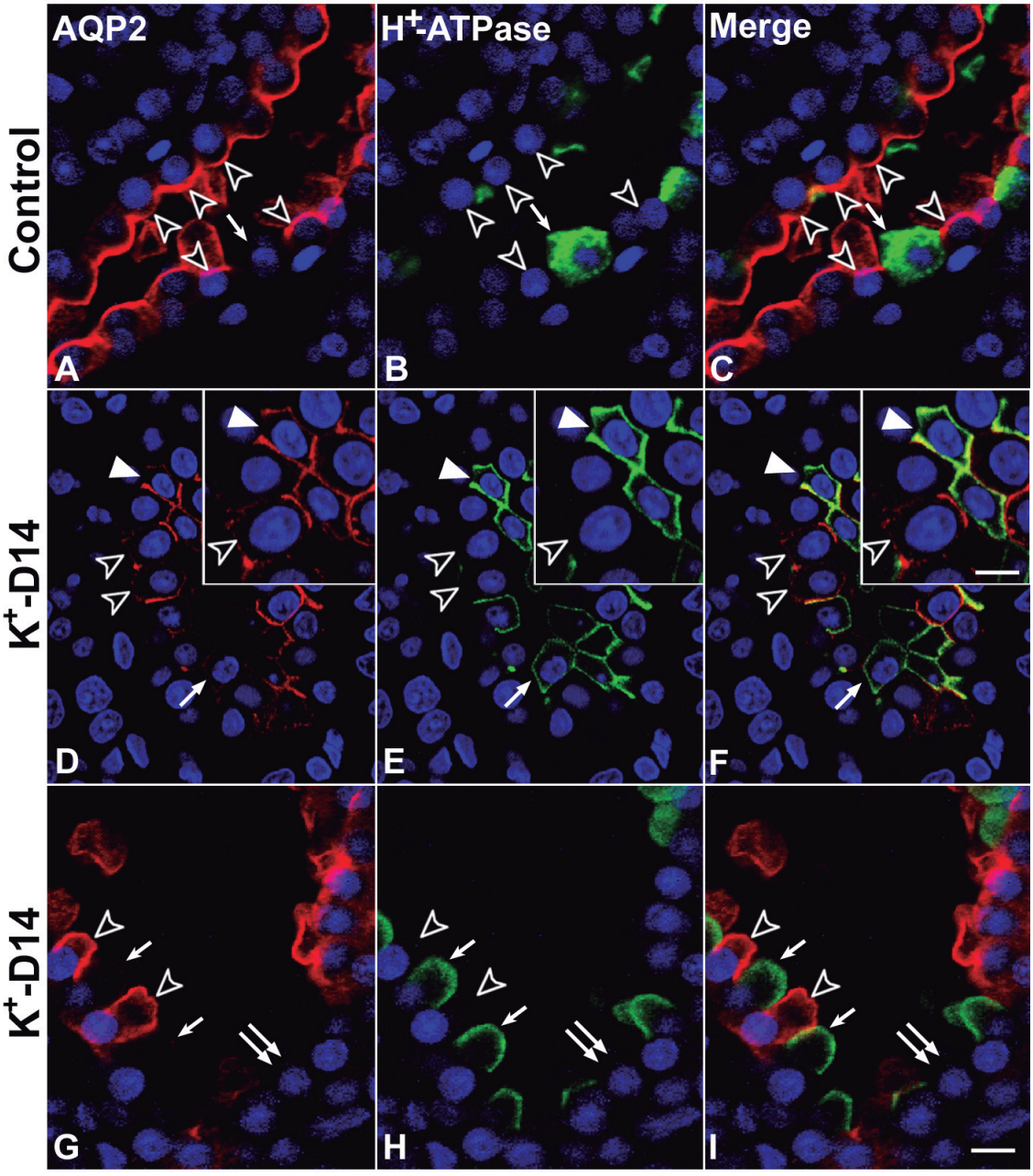

Fig. 9. Confocal micrographs of 50 μm vibratome sections in the ISOM of control **(A-C)** and K^+-D14 **(D-I)** rat kidneys illustrating double immunofluorescence for AQP2 (red) and H^+-ATPase (green). Normally, AQP2 is expressed only in the apical portion of PCs (open arrowheads in **A-I**), and H^+-ATPase is expressed only in the apical portion of ICs (arrows in **A-I**). However, in a few cells, AQP2 and H^+-ATPase were colocalized in the apical portion on K^+-D14 (arrowheads in **D-F**). The inset panel is a high-magnification image of the colocalized cells in **D-F** (arrowheads; bar 5 μm). Some cells did not express either AQP2 or H^+-ATPase on K^+-D14 (double arrows in **G-I**). Bar: 10 μm.

Table 2. Summary of cell counting.

Parameter (per 5mm)	Region	Potassium status	Rat N=	Sections, total no.	Image no.	No. of CDs	No. of cells (% of total cell No.)
AQP2+ cells	ISOM	Control	3	3	45	98	696 (73.42%)
		K^+-D 14	3	3	54	153	634 (59.36%)
		K^+-R 3	3	3	54	138	688 (72.80%)
H^+-ATPase+ cells	ISOM	Control	3	3	45	98	252 (26.58%)
		K^+-D 14	3	3	54	153	412 (38.58%)
		K^+-R 3	3	3	54	138	238 (25.19%)
AQP2 and H^+-ATPase+ cells	ISOM	Control	3	3	45	98	0 (0%)
Intermediate cells		K^+-D 14	3	3	54	153	12 (1.12%)
		K^+-R 3	3	3	54	138	10 (1.06%)
AQP2 and H^+-ATPase- cells	ISOM	Control	3	3	45	98	0 (0%)
Null cells		K^+-D 14	3	3	54	153	10 (0.94%)
		K^+-R 3	3	3	54	138	9 (0.95%)

ISOM, inner stripe of the outer medulla; CD, collecting duct; K^+-D, potassium depletion; K^+-R, potassium repletion.

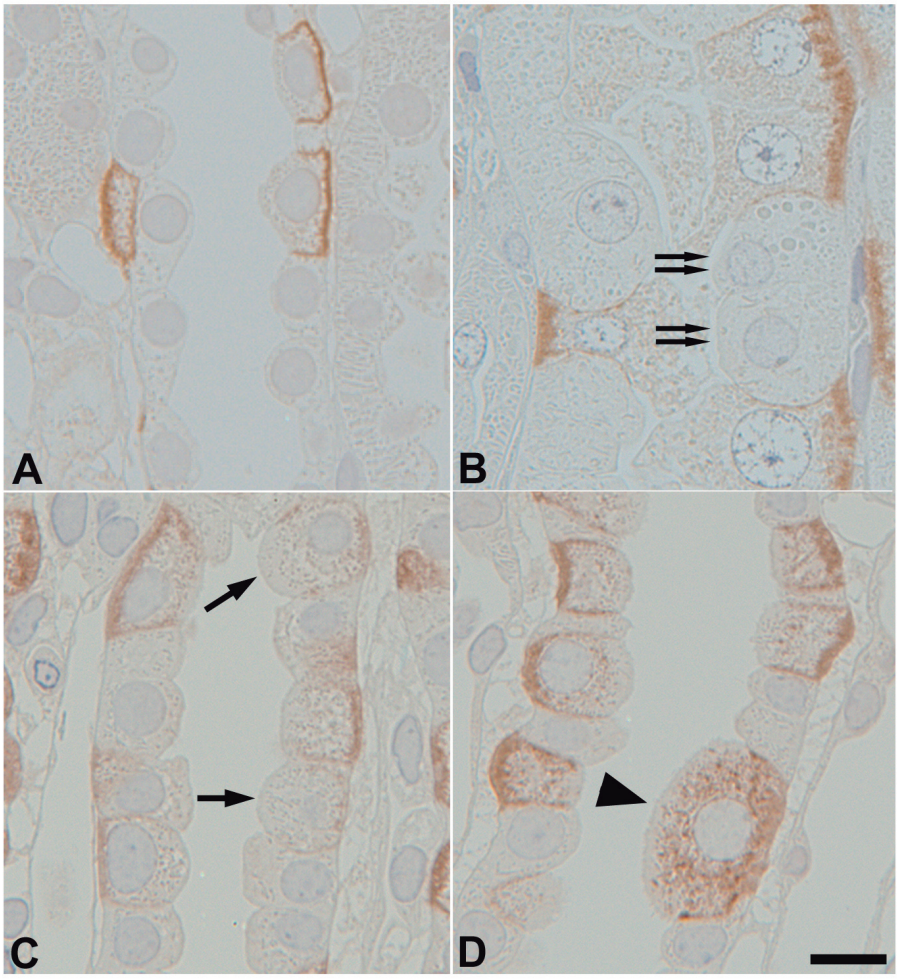

Fig. 10. Light micrographs of 1.5 μm semithin sections in the ISOM of control **(A)**, K^+-D14 **(B)**, and K^+-R3 (**C-D**) rat kidneys illustrating single immunostaining for AE1. **A.** Type A ICs exhibit basolateral AE1 immunolabeling in the control group. **B**. On K^+-D14, highly activated AE1-positive ICs were observed and AE1-negative PCs had many intracellular vesicles (double arrows). **C-D**. On K^+-R3, immunoreactivity for AE1 was markedly reduced (arrows), and immunostaining for AE1 was present in the intracellular structures of some cells (arrowhead). Bar: 10 μm

in ICs on day 3 of K^+-R (Fig. 13E, F).

Discussion

The current study provides important new information regarding the cellular mechanism of renal adaptation to K^+-D and K^+-R. During K^+-D induced with a K^+-free diet there was a reversible increase in the number and proportion of ICs and induction of hyperplasia in the ISOM, but cell proliferation was limited to PCs. During K^+-R there was a decrease in the number and proportion of ICs and induction of apoptosis, but the apoptosis was limited to PCs. Both K^+-D and K^+-R induced expression of 'intermediated' CD cells, with characteristics of both ICs and PCs, and 'null' cells, which lack characteristics of both IC and PC proteins. Finally, K^+-D and K^+-R induce autophagy. These findings suggest that K^+-D and K^+-R alter ISOM

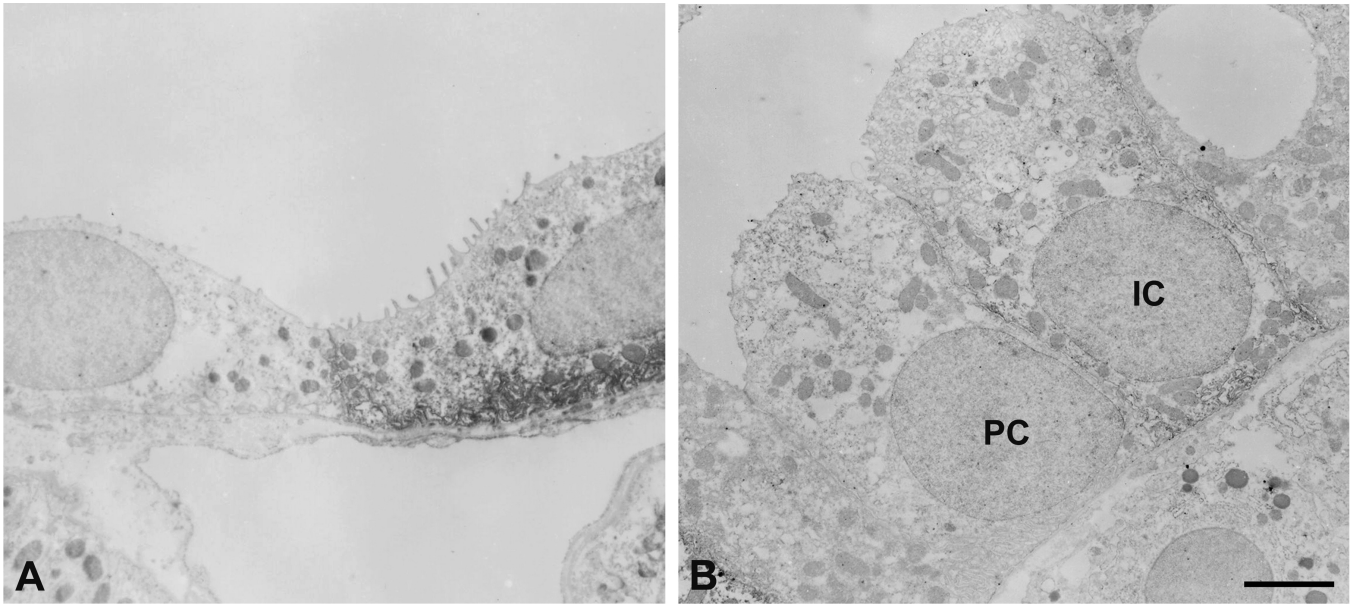

Fig. 11. Electron micrographs of ultrathin sections in the ISOM of control **(A)** and K^+-R3 **(B)** rat kidneys illustrating single immunostaining for AE1. **A.** Type A ICs for basolateral AE1 immunolabeling had apical microplicae and numerous mitochondria in the cytoplasm in control rats. **B.** On K^+-R3, the ultrastructure of type A ICs did not differ from that of PC and AE1 immunolabeling was very weak. Bar: 2 μm

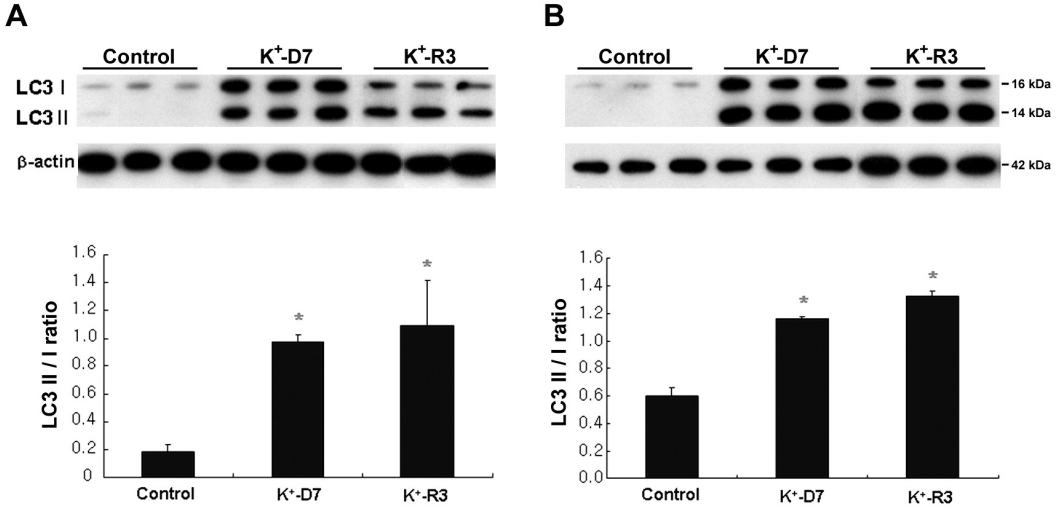

Fig. 12. Immunoblot of LC3I and LC3II in the outer medulla (OM, **A**) and inner medulla (IM, **B**) of control, K^+-D7, and K^+-R3 rat kidneys. **A-B**. The expression of LC3II in the OM and IM was markedly increased on K^+-D7 compared with the control, and was pronounced on K^+-R3. Top: immunoblot image. Bottom: summary of densitometric analysis. Values are expressed as mean ± SE; n=5 rats per group. *P<0.05.

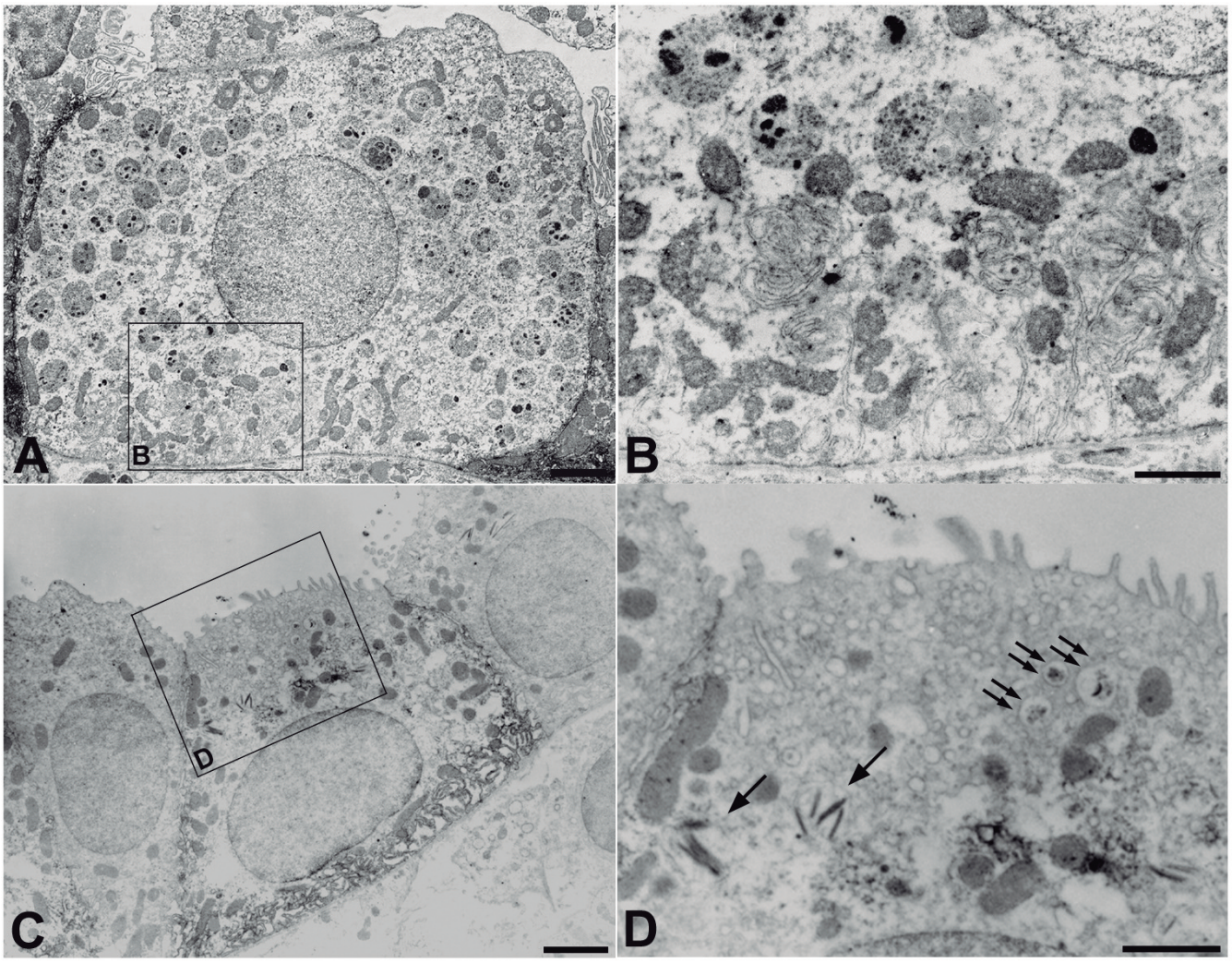

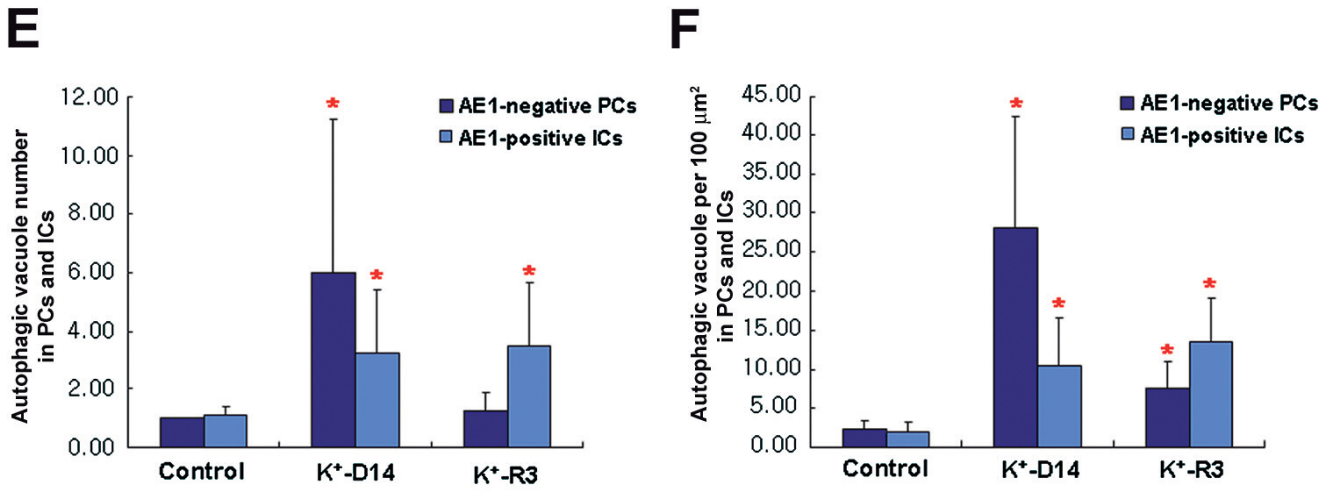

Fig. 13. Electron micrographs of ultrathin sections in the ISOM of K⁺-D14 and K⁺-R3 rat kidneys illustrating single immunostaining for AE1 (**A-D**). Quantification of the number (**E**) and volume (**F**) of autophagic vacuoles (AVs) in the ISOM of control, K⁺-D14, and K⁺-R3. **A-B**. AE1-negative PCs contained many AVs on K⁺-D14. **C-D**. On K⁺-R3 AE1-positive ICs contained many AVs (arrows) and multivesicular bodies (double arrows) in the cytoplasm. **E-F**. The numbers and volumes of AVs were significantly increased on K⁺-D14 and K⁺–R3 compared with the control group. Interestingly, the numbers and volumes of AVs were particularly pronounced in PCs on K⁺-D14, and in ICs on K⁺-R3. *P<0.05. Bars: A, C, 2 μm; B, D, 1 μm.

potassium transport through changes in the number and proportion of ICs, that the changes in the number and proportion of ICs involves epithelial transdifferentiation between ICs and PCs, and that cellular autophagy is involved in this epithelial transdifferentiation.

The renal response to hypokalemia involves adaptations in multiple renal sites. In the proximal tubule there is hypertrophy and increased luminal bicarbonate reabsorption (Rector et al. 1964) that involves, at least in part, increased type 3 Na^+/H^+ exchanger, NHE-3 and Na^+-HCO_3^- cotransporter 1, NBC1 expression (Elkjaer et al., 2002). In the thick ascending limb of the loop of Henle there is decreased Na^+-K^+-$2Cl^-$ cotransporter, and in the distal convoluted tubule there is decreased Na^+-Cl^- cotransporter (Elkjaer et al., 2002). Despite these changes, however, there are only minimal changes in distal nephron K^+ delivery; the major adaptation in renal potassium transport occurs in the CD.

CD potassium transport involves both unidirectional potassium secretion and reabsorption. Potassium secretion involves PC-mediated reabsorption of luminal sodium in parallel with potassium secretion; K^+ secretion occurs through apical small-conductance, ROMK-like K^+ channels and Ca^{2+}-activated, large conductance K^+ (BK) channels (Wang and Giebisch, 2009; Aronson and Giebisch, 2011). K^+-D inhibits both of these apical K^+ transport mechanisms (Wei et al., 2001; Li et al., 2006) and involves a wide variety of signaling mechanisms, including Src, mitogen-activated protein kinase (MAPK), protein tyrosine kinase, superoxide anions, and the angiotensin II type 1 receptor (Lin et al., 2002; Babilonia et al., 2005, 2006). In addition, K^+-D through stimulation of ERK can inhibit epithelial Na^+ channels, thereby decreasing the driving force for K^+ secretion (Soundararajan et al., 2005). This multiplicity of regulatory mechanisms enables adaptive changes in PC unidirectional K^+ secretion despite an absence of change in total number of PCs.

ICs mediate a fundamental role in renal K^+ transport through their ability to actively reabsorb luminal K^+ through apical H^+-K^+-ATPase. Recently, it has been proposed that BK-α/ß4 in ICs has a role in flow-mediated K^+ secretion during K^+ adaptation (Najjar et al., 2005; Holtzclaw et al., 2010; Wang et al., 2010). H^+-K^+-ATPase consists of both an α- and a ß-subunit, and two α-subunits have been identified, a gastric-like, α1-subunit, and a colonic-type, α2-subunit. K^+-D increases H^+-K^+-ATPase enzymatic activity and it increases expression of both α-subunits (Gumz et al., 2010). K^+-D also increases IC-mediated K^+ reabsorption by inhibiting K^+ recycling across the apical plasma membrane and increasing K^+ exit through basolateral Ba^{2+}-sensitive K^+ channels (Zhou and Wingo, 1994; Zhou et al., 2000). The current study adds to our understanding of the mechanisms through which K^+-D increases ISOM K^+ reabsorption by demonstrating increased numbers of ICs in response to dietary K^+ restriction.

Several previous studies have addressed the issue as to whether there are changes in the number of the different CD cells, PCs versus ICs, in response to hypokalemia. Several studies, including the current study, have shown increased numbers of ICs (Oliver et al., 1957; Ordonez et al., 1977), whereas others have shown no changes in the number of either ICs or PCs (Hansen et al., 1980; Stetson et al., 1980). One possible explanation for these different results may relate to different criteria and methods used to identify ICs and PCs in different studies. In particular, the identification, for the first time, in the current study of both 'intermediate' and 'null' CD cells, may have complicated the assessment of the actual number of 'true' ICs and PCs in studies using alternative identification techniques.

Whether CD cells can undergo epithelial transdifferentiation has been a controversial issue in renal physiology. Chronic lithium exposure induces polyuria and decreased collecting duct responsiveness to AVP, and is associated with decreased numbers of PCs and increased numbers of ICs (Christensen et al., 2004). Subsequent studies identified that lithium induced proliferation of CD cells in the IM, and that the proliferation preferentially was present in non-ICs, specifically the inner medullary collecting duct (IMCD) cell, rather than in ICs (Christensen et al., 2006). They suggested that in the conversion of PCs to ICs, ICs may have arisen directly from the differentiation of PCs to ICs (Christensen et al., 2006). Recently, it was proposed that a change in the fractional contribution of a specific cell type does not necessarily require active proliferation of the congeneric cell type in a heterogeneous cell population (Wehrli et al., 2007). Altered cell proliferation may contribute to cellular remodeling of CD in response to systemic acid/base homeostasis (Yasoshima et al., 1992; Tsuruoka and Schwartz, 1996; Wehrli et al., 2007). If this is possible, it would be expected that one would see some cell-like 'intermediate' cells with both the IC marker, H^+-ATPase, and the PC marker, AQP4, when cell conversion had occurred between PCs and ICs (Christensen et al., 2006). However, in contrast to the current study, 'intermediate' cells, which provide direct evidence for epithelial transdifferentiation of PCs into ICs, was not identified. Interconversion (epithelial transdifferentiation) could also explain that the changes of cellular composition reverse after K^+-R, and the ICs convert back to PCs.

Another possibility is consistent with a recent study that suggests ICs may arise from a common progenitor cell. Similar to the current study, rare 'null' cells, lacking phenotypic expression of both H^+-ATPase and AQP4, were present (Christensen et al., 2006). These cells may have entered the collecting duct to produce ICs in the lithium treatment differently from the absence in control rats (Christensen et al., 2006). A type of progenitor/stem cell could have differentiated into ICs (Christensen et al., 2006). Several studies on lithium treatment identified cells that were negative for both PC and IC markers using double immunolabeling, but the fractional contribution of these all-negative cells was very low

(<1%), which is consistent with our result (Christensen et al., 2004, 2006). These cells entered the collecting duct and may have given rise to ICs during lithium treatment, differently from the absence in control rats (Christensen et al., 2006). They might be a type of progenitor/stem cell that can differentiate into an IC (Christensen et al., 2006; Ecelbarger, 2006). We think that the existence of cells that lack staining for all markers is an important result even though these null cells were few in number. A recent study with mice lacking the forkhead transcription factor Foxi1 suggested that Foxi1 is required for the differentiation of precursor cells into ICs and that Foxi1 regulates the expression of IC-specific genes, AE1 and Pendrin (Blomqvist et al., 2004). Moreover, Jeong et al. (2009) demonstrated from mice lacking Mind bomb-1 in the renal CD that Notch signaling inhibits the function of Foxi1 directly or indirectly for the proper differentiation into PCs. In metabolic acidosis some studies have identified increased numbers of type A ICs in conjunction with decreased numbers of type B ICs, without evidence of IC hyperplasia, with a simultaneous increase in the number of AQP2-positive PCs (Purkerson et al., 2010). In contrast, another study reported that metabolic acidosis increased the number of ICs and decreased the proportion of PCs and identified induction of hyperplasia in ICs (Van Huyen et al., 2008; Welsh-Bacic et al., 2011). Finally, chronic carbonic anhydrase inhibition appears to decrease the number of type B ICs and increase the number of type A ICs in the rat cortical collecting duct (CCD), and to increase the number of ICs in the outer medullary collecting duct (OMCD) and to decrease the number in the IMCD (Bagnis et al., 2001), although whether these effects, at least in the CCD and OMCD, were secondary to induction of chronic metabolic acidosis or were specific, pH-independent effects of carbonic anhydrase inhibition is unclear, as ICs in the OMCD also showed phenotypic changes associated with the response to metabolic acidosis (Bagnis et al., 2001). In contrast, other studies have found no evidence of change in CD cellular composition with either metabolic acidosis or hypokalemia (Hansen et al., 1980; Verlander et al., 1996).

The current study is the first study to provide direct evidence in an *in vivo* model that interconversion between ICs and PCs occurs and likely mediates an important role in regulated ion transport. Multiple lines of evidence support interconversion between PCs and ICs. K^+-D increases the number and proportion of ICs in the ISOM, but induces proliferation only in PCs. Simultaneously, there is induction of 'intermediate' cells with characteristics of both ICs, namely H^+-ATPase and AE1 immunolabel, and PCs, AQP2 immunolabel expression. The number of 'intermediate' cells is physiologically regulated, increasing at times of changes in the relative number and proportion of ICs and PCs. With K^+-R there is a decrease in the number and proportion of ICs and an induction of CD apoptosis, but the apoptosis is present almost exclusively in PCs. Supporting interconversion of ICs into PCs is the identification of cells with both ICs and PCs phenotypic characteristics using both immunohistochemistry criteria and immunoelectron microscopy criteria. Moreover, the presence of interconversion explains the observation that cellular proliferation and removal, during K^+-D and K^+-R, respectively, is limited to PCs, whereas changes in the total number of cells is limited to the IC population. In a previous study Fejes-Tóth and Náray-Fejes-Tóth observed hybrid cells expressing both type B IC and PC antigens in primary culture and suggested that this indicated cellular conversion of ICs and PCs (Fejes-Tóth and Náray-Fejes-Tóth, 1992). Thus, the presence of 'intermediate' cells that exhibited markers characteristic of both ICs and PCs in our *in vivo* study is consistent with the concept of cellular interconversion *in vitro*, as described earlier (Fejes-Tóth and Náray-Fejes-Tóth, 1992). Recently, the review suggested that the routes to regeneration in the lens propose the processes of dedifferentiation and transdifferentiation (Jopling et al., 2011). The possible mechanism described that cells undergo dedifferentiation to a precursor stage before it can enter the new lineage or cells directly transdifferentiate to form the new cells, in some cases passing through an unnatural intermediate phase in which two genetic programmes are active at the same time (Jopling et al., 2011). Another possible mechanism for the increase in type A ICs is the conversion of type B IC to type A IC, a process that is modulated by an extracellular protein called hensin (Schwartz et al., 1985; Al-Awqati, 2008; Gao et al., 2010). However, in our study, no type B ICs were observed in the inner stripe of the OMCD neither in the control animals nor in the experimental animals.

Autophagy is a normal physiologic process involved in the cellular degradation of long-lived proteins as well as in organelle turnover. It is often induced as an integral component of the cellular response to physiological stimuli, such as nutrient starvation, control of cellular growth and intracellular protein turnover (Mizushima, 2005; Periyasamy-Thandavan et al., 2009). Renal epithelial responsiveness to fluid and electrolyte disorders often involves the production of proteins involved in ion transport; presumably there is also degradation of these proteins when the stimulus is no longer present. The signal which initiates and/or regulates autophagy in the renal response to dietary K^+ alterations is unclear, but may involve the MAPK signaling system, which is activated both in response to K^+-D (Jin et al., 2009; Wang et al., 2010), and in other models of autophagy (Roux and Blenis, 2004; Corcelle et al., 2007). The current study is the first to show evidence for involvement of autophagy in renal fluid and electrolyte homeostasis, in particular, in the response to changes in dietary K^+ availability.

Accumulation of autophagic vacuoles occurs mainly in PCs during K^+-D and in ICs during K^+-R, suggesting that autophagy could be involved in maintaining cell numbers, even though there is a proliferation of PCs

during K^+-D and a reduction in the number of ICs during K^+-R. Moreover, this process appears to be temporally associated with epithelial transdifferentiation between ICs and PCs, suggesting that autophagic degradation of proteins specific to differentiated ICs or PCs functions contribute to epithelial transdifferentiation and to adaptive changes in cellular function.

In summary, K^+-D induced hypertrophy and hyperplasia of the CD, especially in ICs, and K^+-R normalized these changes. However, cell proliferation during K^+-D and apoptosis during K^+-R was mainly observed in PCs. The identification of 'intermediate' cells, both by immunohistochemistry and by immune-ultrastructural criteria, suggests that interconversion between ICs and PCs in response to changes in K^+ availability both occurred, and was central to the changes in the CD cell-type numbers that were observed. Thus, these findings indicate that PCs and ICs may interconvert in CD remodeling during potassium homeostasis and that autophagic pathways may be involved in the interconversion.

Acknowledgements. This research was supported by Basic Science Research Program through the National Research Foundation of Korea (NRF) funded by the Ministry of Education, Science and Technology (20110023141).

Disclosures. None.

References

Aronson P.S. and Giebisch G. (2011). Effects of pH on potassium: new explanations for old observations. J. Am. Soc. Nephrol. 22, 1981-1989.

Al-Awqati Q. (2008). 2007 Homer W. Smith award: control of terminal differentiation in epithelia. J. Am. Soc. Nephrol. 19, 443-449.

Babilonia E., Wei Y., Sterling H., Kaminski P., Wolin M. and Wang W.H. (2005). Superoxide anions are involved in mediating the effect of low K intake on c-Src expression and renal K secretion in the cortical collecting duct. J. Biol. Chem. 280, 10790-10796.

Babilonia E., Li D., Wang Z., Sun P., Lin D.H., Jin Y. and Wang W.H. (2006). Mitogen-activated protein kinases inhibit the ROMK (Kir 1.1)-like small conductance K channels in the cortical collecting duct. J. Am. Soc. Nephrol. 17, 2687-2696.

Bagnis C., Marshansky V., Breton S. and Brown D. (2001). Remodeling the cellular profile of collecting ducts by chronic carbonic anhydrase inhibition. Am. J. Physiol. Renal Physiol. 280, F437-F448.

Bailey M.A., Fletcher R.M., Woodrow D.F., Unwin R.J. and Walter S.J. (1998). Upregulation of H^+-ATPase in the distal nephron during potassium depletion: structural and functional evidence. Am. J. Physiol. Renal Physiol. 275, F878-F884.

Blomqvist S.R., Vidarsson H., Fitzgerald S., Johansson B.R., Ollerstam A., Brown R., Persson A.E., Bergstrom G.G. and Enerback S. (2004). Distal renal tubular acidosis in mice that lack the forkhead transcription factor Foxi1. J. Clin. Invest. 113, 1560–1570.

Christensen B.M., Marples D., Kim Y.H., Wang W., Frokiaer J. and Nielsen S. (2004). Changes in cellular composition of kidney collecting duct cells in rats with lithium-induced NDI. Am. J. Physiol. Cell Physiol. 286, C952-C964.

Christensen B.M., Kim Y.H., Kwon T.H. and Nielsen S. (2006). Lithium treatment induces a marked proliferation of primarily principal cells in rat kidney inner medullary collecting duct. Am. J. Physiol. Renal Physiol. 291, F39-F48.

Corcelle E., Djerbi N., Mari M., Nebout M., Fiorini C., Fenichel P., Hofman P., Poujeol P. and Mograbi B. (2007). Control of the autophagy maturation step by the MAPK ERK and p38: lessons from environmental carcinogens. Autophagy 3, 57-59.

Ecelbarger C.A. (2006). Lithium treatment and remodeling of the collecting duct. Am. J. Physiol. Renal Physiol. 291, F37-F38.

Elger M., Bankir L. and Kriz W. (1992). Morphometric analysis of kidney hypertrophy in rats after chronic potassium depletion. Am. J. Physiol. Renal Physiol. 262, F656-F667.

Elkjaer M.L., Kwon T.H., Wang W., Nielsen J., Knepper M.A., Frøkiaer J. and Nielsen S. (2002). Altered expression of renal NHE3, TSC, BSC-1, and ENaC subunits in potassium-depleted rats. Am. J. Physiol. Renal Physiol. 283, F1376-F1388.

Fejes-Tóth G and Náray-Fejes-Tóth A. (1992). Differentiation of renal beta-intercalated cells to alpha-intercalated and principal cells in culture. Proc. Natl. Acad. Sci. USA 89, 5487-5491.

Gao X., Eladari D., Leviel F., Tew B.Y., Miro-Julia C., Cheema F., Miller L., Nelson R., Paunescu T.G., Mckee M., Brown D. and Al-Awqti Q. (2010). Deletion of hensin/DMBT1 blocks conversion of ,- to ·- intercalated cells and induces distal renal tubular acidosis. Proc. Natl. Acad. Sci. USA 107, 21872-21877.

Giebisch G., Hebert S.C. and Wang W.H. (2003). New aspects of renal potassium transport. Pflugers Arch. 446, 289-297.

Gumz M.L., Lynch I.J., Greenlee M.M., Chin B.D. and Wingo C.S. (2010). The renal H^+-K^+-ATPases: physiology, regulation, and structure. Am. J. Physiol. Renal Physiol. 298, F12-F21.

Han K.H., Lee S.Y., Kim W.Y., Shin J.A., Kim J. and Weiner I.D. (2010). Expression of ammonia transporter family members, Rh B glycoprotein and Rh C glycoprotein, in the developing rat kidney. Am. J. Physiol. Renal Physiol. 299, F187-F198.

Hansen G.P., Tisher C.C. and Robinson R.R. (1980). Response of the collecting duct to disturbances of acid-base and potassium balance. Kidney Int. 17, 326-337.

Holtzclaw J.D., Grimm P.R. and Sansom S. (2010). Intercalated cell BK-a/ß4 channels modulate sodium and potassium handling during potassium adaptation. J. Am. Soc. Nephrol. 21, 634-645.

Jeong H.W., Jeon U.S., Koo B.K., Kim W.Y., Im S.K., Shin J., Cho Y., Kim J. and Kong Y.Y. (2009). Inactivation of Notch signaling in the renal collecting duct causes nephrogenic diabetes insipidus in mice. J. Clin. Invest. 119, 3290–3300.

Jin Y., Wang Y., Wang Z.J., Lin D.H. and Wang W.H. (2009). Inhibition of angiotensin type 1 receptor impairs renal ability of K conservation in response to K restriction. Am. J. Physiol. Renal Physiol. 296, F1179-F1184.

Jopling D., Stephanie B. and Izpisua Belmonte J.C. (2011). Differentiation, transdifferentiation and reprogramming: three routes to regeneration. Nat. Rev. Mol. Cell Biol. 12, 79-89.

Kim J., Tisher C.C. and Madsen K.M. (1994). Differentiation of ICs in developing rat kidney: An immunohistochemical study. Am. J. Physiol. Renal Physiol. 266, F977–F990.

Kim J., Kim Y.H., Cha J.H., Tisher C.C. and Madsen K.M. (1999). IC subtypes in connecting tubule and cortical collecting duct of rat and mouse. J. Am. Soc. Nephrol. 10, 1-12.

Kim J., Cha J.H., Tisher C.C. and Madsen K.M. (2000). Role of apoptotic and nonapoptotic cell death in removal of intercalated cells

from developing rat kidney. Am. J. Physiol. Renal Physiol. 270, F575-F592.

Kim Y.H., Kwon T.H., Frische S., Kim J., Tisher C.C., Madsen K.M. and Nielsen S. (2002). Immunocytochemical localization of pendrin in IC subtypes in rat and mouse kidney. Am. J. Physiol. Renal Physiol. 283, F744 –F754.

Kim W.Y., Jung J.H., Park E.Y., Yang C.W., Kim H., Nielsen S., Madsen K.M. and Kim J. (2006). Expression of protein kinase C isoenzymes alpha, betaI, and delta in subtypes of intercalated cells of mouse kidney. Am. J. Physiol. Renal Physiol. 291, F1052-F1060.

Kim W.Y., Kim Y.H., Park E.Y., Hwang J.S., Kim Y.M. and Kim J. (2008). Expression of aquaporin-3 and aquaporin-4 in aquaporin-1 knockout mice. The Korean J. Anat. 41, 163-172.

Kimura T., Nishino T., Maruyama N., Hamano K., Kubo A., Iwano M. and Shiiki H. (2001). Expression of Bcl-2 and Bax in hypokalemic nephropathy in rats. Pathobiology 69, 237-248.

Lee H.W., Kim W.Y., Song H.K., Yang C.W., Han K.H., Kwon H.M. and Kim J. (2007). Sequential expression of NKCC2, TonEBP, aldose reductase, and urea transporter-A in developing mouse kidney. Am. J. Physiol. Renal Physiol. 292, F269-F277.

Li D., Wang Z., Sun P., Jin Y., Lin D.H., Hebert S.C., Giebisch G. and Wang W.H. (2006). Inhibition of MAPK stimulates the Ca2+-dependent big-conductance K channels in cortical collecting duct. Proc. Natl. Acad. Sci. USA 103, 19569-19574.

Lin D.H., Sterling H., Lerea K.M., Welling P., Jin L., Giebisch G. and Wang W.H. (2002). K depletion increases protein tyrosine kinase-mediated phosphorylation of ROMK. Am. J. Physiol. Renal Physiol. 283, F671-F677.

Mizushima N. (2005). The pleiotropic role of autophagy: from protein metabolism to bactericide. Cell Death Differ. 12, 1535-1541.

Muto S. (2001). Potassium transport in the mammalian collecting duct. Physiol. Rev. 81, 85-116.

Najjar F., Zhou H., Morimoto T., Bruns J.B., Li H.S., Liu W., Kleyman T.R. and Satlin L.M. (2005). Dietary K^+ regulates apical membrane expression of maxi-K channels in rabbit cortical collecting duct. Am. J. Physiol. Renal Physiol. 289, F922-F932.

Oliver J., MacDowell M., Welt L.G., Holliday M.A., Hollander J., Winters R.W., Williams T.F. and Segar W.E. (1957). The renal lesions of electrolyte imbalance. I. The structural alterations in potassium-depleted rats. J. Exp. Med. 106, 563-574.

Ordonez N.G., Toback F.G., Aithal H.N. and Spargo B.J. (1977). Zonal changes in renal structure and phospholipid metabolism during reversal of potassium depletion nephropathy. Lab. Invest. 36, 33-47.

Periyasamy-Thandavan S., Jiang M., Schoenlein P. and Dong Z. (2009). Autophagy: molecular machinery, regulation, and implications for renal pathophysiology. Am. J. Physiol. Renal Physiol. 297, F244-F256.

Purkerson J.M., Tsuruoka S., Suter D.Z., Nakamori A. and Schwartz G.J. (2010). Adaptation to metabolic acidosis and its recovery are associated with changes in anion exchanger distribution and expression in the cortical collecting duct. Kidney Int. 78, 993-1005.

Rector F.C. Jr, Bloomer H.A. and Seldin D.W. (1964). Effect of potassium deficiency on the reabsorption of bicarbonate in the proximal tubule of the rat kidney. J. Clin. Invest. 43, 1976-1982.

Roux P.P. and Blenis J. (2004). ERK and p38 MAPK-activated protein kinases: a family of protein kinases with diverse biological functions. Microbiol. Mol. Biol. Rev. 68, 320-344.

Schwartz G.J., Barasch J. and Al-Awqati Q. (1985). Plasticity of functional epithelial polarity. Nature 318, 368-371.

Silver R.B., Breton S. and Brown D. (2000). Potassium depletion increases proton pump (H^+-ATPase) activity in intercalated cells of cortical collecting duct. Am. J. Physiol. Renal Physiol. 279, F195-F202.

Song H.K., Kim W.Y., Lee H.W., Park E.Y., Han K.H., Nielsen S., Madsen K.M. and Kim J. (2007). Origin and fate of pendrin-positive intercalated cells in developing mouse kidney. J. Am. Soc. Nephrol. 18, 2672-2682.

Soundararajan R., Zhang T.T., Wang J., Vandewalle A. and Pearce D. (2005). A novel role for glucocorticoid-induced leucine zipper protein in epithelial sodium channel-mediated sodium transport. J. Biol. Chem. 280, 39970-39981.

Stetson D.L., Wade J.B. and Giebisch G. (1980). Morphologic alterations in the rat medullary collecting duct following potassium depletion. Kidney Int. 17, 45-56.

Toback F.G., Ordónez N.G., Bortz S.L. and Spargo B.H. (1976). Zonal changes in renal structure and phospholipid metabolism in potassium-deficient rats. Lab. Invest. 34, 115-124.

Toyoshima H. and Watanabe T. (1988). Rapid regression of renal medullary granular change during reversal of potassium depletion nephropathy. Nephron 48, 47-53.

Tsuruoka S. and Schwartz G.J. (1996). Adaptation of rabbit cortical collecting duct HCO3- transport to metabolic acidosis *in vitro*. J. Clin. Invest. 97, 1076-1084.

Van Huyen J.P.D., Cheval L., Bloch-Faure M., Belair M.F., Heudes D., Bruneval P. and Doucet A. (2008). GDF15 triggers homeostatic proliferation of acid-secreting collecting duct cells. J. Am. Soc. Nephrol. 19, 1965-1974.

Verlander J.W., Madsen K.M. and Tisher C.C. (1996). Axial distribution of band 3-positive intercalated cells in the collecting duct of control and ammonium chloride-loaded rabbits. Kidney Int. 57 (Suppl. 57), S137-S147.

Wang W.H. and Giebisch G. (2009). Regulation of potassium (K) handling in the renal collecting duct. Pflugers Arch. 458, 157-168.

Wang Z.J., Sun P., Xing W., Pan C., Lin D.H. and Wang W.H. (2010). Decrease in dietary K intake stimulates the generation of superoxide anions in the kidney and inhibits K secretory channels in the CCD. Am. J. Physiol. Renal Physiol. 298, F1515-F1522.

Wehrli P., Loffing-Cueni D., Kaissling B. and Loffing J. (2007). Replication of segment-specific and intercalated cells in the mouse renal collecting system. Histochem. Cell Biol. 127, 389-398.

Wei Y, Bloom P., Gu R. and Wang W.H. (2001). Effect of dietary K intake on apical small-conductance K channel in CCD: role of protein tyrosine kinase. Am. J. Physiol. Renal Physiol. 281, F206-F212.

Welsh-Bacic D., Nowik M., Kaissling B. and Wagner C.A. (2011). Proliferation of acid-secretory cells in the kidney during adaptation remodeling of the collecting duct. PLoS ONE 6, e25240.

Yasoshima K., Satlin L.M. and Schwartz G.J. (1992). Adaptation of rabbit cortical collecting duct to *in vitro* acid incubation. Am. J. Physiol. 263, F749-F756.

Zhou X. and Wingo C.S. (1994). Stimulation of total CO_2 flux by 10% CO_2 in rabbit CCD: role of an apical Sch-28080- and Ba-sensitive mechanism. Am. J. Physiol. 267, F114-F120.

Zhou X., Lynch I.J., Xia S.L. and Wingo C.S. (2000). Activation of H^+-K^+-ATPase by CO2 requires a basolateral Ba^{2+}-sensitive pathway during K restriction. Am. J. Physiol. Renal Physiol. 279, F153-F160.

Accepted June 20, 2012